This is to certify that the

thesis entitled

Electrochemical Oxidation and Characterization
of μ-Oxo-(Tetra-T-Butylphthalocyaninato)
Silicon

presented by

David Gale

has been accepted towards fulfillment
of the requirements for

Master's degree in Chemistry

John C. Cavendish
Major professor

Date 8-9-89

ELECTROCHEMICAL OXIDATION AND CHARACTERIZATION OF μ-OXO-(TETRA-T-BUTYLPHTHALOCYANINATO)SILICON.

by

David C. Gale

A DISSERTATION

Submitted to

Michigan State University

In partial fulfillment of the requirements

for the degree of

MASTER OF SCIENCE

Department of Chemistry

1989

ABSTRACT

ELECTROCHEMICAL OXIDATION AND CHARACTERIZATION OF

μ-OXO-(TETRA-T-BUTYLPHTHALOCYANINATO)SILICON.

by

David C. Gale

The oxidative redox properties of μ-oxo-(tetra-t-butylphthalocyaninato)silicon was investigated in solution by conventional electrochemical techniques. This soluble, covalently-linked polymer, a known electrical conductor in the solid state when oxidized (doped), was characterized using controlled potential coulometry (CPC), rotating disk voltammetry (RDE), differential pulse voltammetry (DPV), and cyclic voltammetry (CV). Digital simulations of the voltammetry results were performed to obtain information regarding the potential of redox sites comprising the polymer. The degree of partial oxidation can be adjusted to any level ranging from zero to 100% (from neutral material to one electron removed per phthalocyanine site). This process occurs over a 1700 mV range and is consistent for a material with a large amount of interaction between adjacent molecules. Voltammetry experiments and spectroscopic measurements indicate that the doped material is stable at all degrees of partial oxidation. RDE results suggest that there is no kinetic limitation for the oxidative process, allowing the thermodynamic potentials for band depletion to be accurately determined.

To My Parents

ACKNOWLEDGEMENTS

The author would like to thank all of the people who have provided assistance on this project. I would like to thank my parents for all of their support, understanding, and help through the years. I would like to thank my brothers, Peter and Colin, for their advice and encouragement these past few years. I would also like to thank my fellow group members for their helpful suggestions and timely advice. The author greatly appreciates the work of Tom Chapaton regarding the computer simulations. I would like to thank the rest of the graduate students in the department for their friendship, support, and external activities which have made graduate school bearable. Finally, I would like to thank Professor John Gaudiello, for his support during this work, for all the knowledge I have obtained in conversations with him, without his support this project would have never been accomplished.

TABLE OF CONTENTS

page #

page #

LIST OF TABLES

page #

LIST OF SCHEMES

page #

LIST OF FIGURES

Figure page #

Figure page #

Figure page #

1. INTRODUCTION

Organic, organometallic, and inorganic materials that can become electrically conductive upon partial oxidation or reduction (doping) are currently an area of considerable interest.[1] In the 1960's and 1970's, scientists discovered that doped polymers and various condensed organic solids could become metal-like electrical conductors.[2] The development of these materials for use as possible electronic devices has attracted widespread interest and investment in recent years.[3] These doped polymers and condensed organic solids have properties normally associated with traditional metals, that is, the electrical conductivity of these materials goes up as the temperature goes down. These "molecular metals" have generally been grouped into two separate classes. The first class are the molecular solids,[1,4] such as TTF-TCNQ (tetrathiafulvalene-tetracyanoquinodimethane), which are comprised of discrete molecular components that have been condensed into a segregated, organized framework. Molecular solids can usually be redissolved to yield their neutral molecular components. The second class of "molecular metals" is the conducting polymers,[1,5] such as polyacetylene and polythiophene, which are based upon covalently bonded aromatic hydrocarbons or heterocycles. Although there are similarities between these two classes of materials,[6] many of their novel properties are different. Polymers historically have been utilized as insulators for a number of applications in the consumer and

electronics field.[3] Recently electrically conductive polymers have been used in the construction of battery anodes and cathodes, chemical sensors, and electromagnetic interference shielding devices.[3] It has been suggested that these materials will appear in numerous applications because of their light weight, flexibility, and electrical properties.[3c] Although it is no longer believed that these materials will replace conventional metals or semiconductors, they will find specialty applications due to their unique and novel properties. Some of the proposed applications for these materials include use in photoelectrochromic displays, rechargeable batteries, and microelectronic conductive components.[3] It is their unique and novel properties which need to be studied and comprehended before more applications can be made.

All materials can be grouped into one of three classes based on their electrical conductivity, either as a metal, semiconductor, or insulator.[4a] Metals such as copper or silver have electrical conductivities of 10^6 ohm^{-1} cm^{-1}. The electrical conductivity of metals decreases with increasing temperature. This is due to a greater number of lattice vibrations or phonons at increased temperatures which perturb the movement of the mobile charge carriers. Semiconductors typically have electrical conductivities in the range from 10^2 ohm^{-1} cm^{-1} to 10^{-5} ohm^{-1} cm^{-1}. The electrical conductivity of semiconductors increases with increasing temperature. Thermal excitation enables charge carriers to be excited up to the empty valence band from the occupied conduction band, this process increases both the number of charge carriers and the electrical conductivity. The third class of electrical conductors is the

insulators, such as teflon or sulfer, with electrical conductivities less than 10^{-6} ohm^{-1} cm^{-1}. Insulators have completely filled conduction bands and completely empty valence bands similar to semiconductors. However, the band gap or energy difference between the conduction and valence bands is substantial, preventing the movement of electrons from the conduction to the valence band. Neutral or undoped organic polymers are classified as insulators due to their extremely low electrical conductivity. Doped polymers can have electrical conductivities[4a,5] ranging from 10^{-9} to 10^{4} ohm^{-1} cm^{-1}, which spans the entire range of conductivity from insulators to metals. Charge transfer salts typically have conductivities ranging from 10^{1} ohm^{-1} cm^{-1} to 10^{5} ohm^{-1} cm^{-1} which are the conductivities associated with traditional semiconductors and metals.[4] Both charge transfer salts and doped polymers have electrical conductivities associated with semiconductors and insulators, however only from temperature-conductivity and spectroscopic measurements can their electrical classification be determined. The electrical conductivity of doped polymers and most molecular charge-transfer salts goes up as the temperature goes down. This electrical conductivity vs. temperature behavior is similar to that observed for metals.

Both molecular solids and doped conducting polymers have some common features. Both classes of materials exhibit anisotropic, or low-dimensional properties.[6] Electrical conductivity is greater in one direction than in others. In molecular solids, the direction of greatest conductivity is parallel to the stacking axis of the crystal. For conducting polymers, conductivity is greatest along the chain direction. Another common feature for both class of materials

is that they are partially oxidized or reduced when they are electrically conductive. For conducting polymers, charge is transferred between the polymer chain and a dopant (oxidizing or reducing agent, or electrode). In molecular solids, charge is transferred between the donor and acceptor components of the condensed complex. Both classes of "molecular metals" possess two important properties that give rise to their unique characteristics. First, they have a band type electronic structure formed from the closely spaced interacting molecules[4a,7] and second, a partial or fractional oxidation state.[6,8] For example, in a single molecule described by Hückel theory, two single occupied p atomic orbitals can interact to form two molecular orbitals (Figure 1). The two molecular orbitals are a filled low-energy π-bonding orbital and an empty high energy π^*-antibonding orbital. If two molecules are stacked directly on top of one another, such that their molecular orbitals interact, two new filled π-bonding molecular orbitals are formed and are separated in energy by 2t, where t is the tight binding integral a measure of the interaction between the two molecular orbitals (analogous to β, the Hückel integral). Similar to the two new π-bonding molecular orbitals, two new empty π^*-antibonding molecular orbitals are formed also separated by an energy gap of. If a stack of N molecules interact, there will be N π states in the highest occupied molecular orbital band (HOMO) and N π^* states in the lowest unoccupied molecular orbital band (LUMO). A band type electronic structure is formed when the energy difference between these states becomes small. For a filled band (HOMO) comprised of N states, there are 2N electrons occupying the band. A material with a

Figure 1. Band formation from the mixing of electronic states. According to Huckel theory, if two atomic orbitals interact, two molecular orbitals are formed with an energy separation of 2β. If two molecular orbitals interact, then two sets of molecular orbitals are formed. The molecular orbitals in each set are separated in energy by 2t, where t is the transfer integral (a measure of the amount of interaction between adjacent molecules). If n molecules interact, n states are formed, from each of the π and π^* molecular orbitals. Into each band of N states, can be placed 2N electrons.

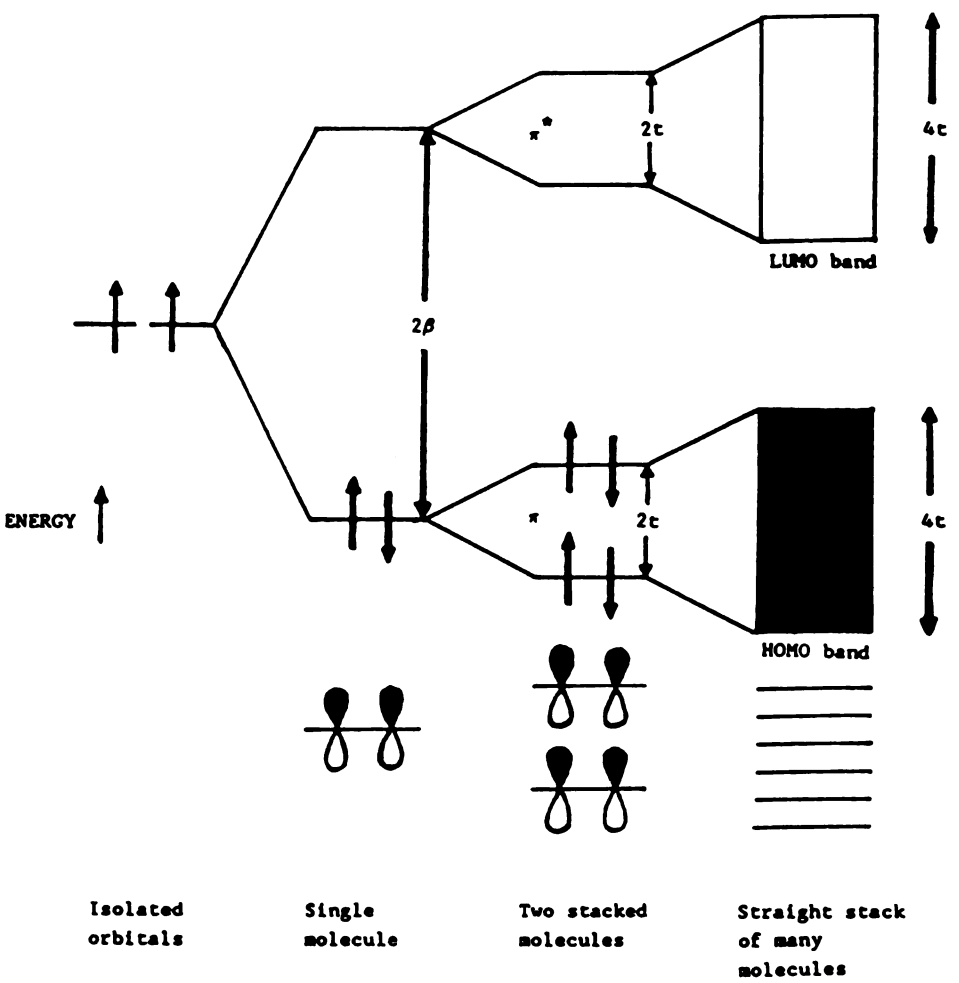
ENERGY
2β
π*
2t
4t
LUMO band
π
2t
4t
HOMO band
Isolated orbitals
Single molecule
Two stacked molecules
Straight stack of many molecules

FIGURE 1

completely filled HOMO band and completely empty LUMO band will be either a semiconductor or an insulator depending on the energy separation between the two bands and the temperature. The second property that conducting polymers and charge transfer salts possess, is a fractional or partial oxidation state where the HOMO or LUMO bands are only partially filled. These fractionally filled bands allow conduction within the band and do not require the transfer of charge between them. The partial filling of these bands can be accomplished by several methods. In molecular charge-transfer salts, charge is usually transferred between the donors and the acceptors. Conducting polymers can be doped either through chemical or electrochemical means.

Neutral conjugated organic polymers are generally insulators or semiconductors due to the lack of charge carriers.[5] Some conjugated polymers have the necessary band type electronic structure arising from the overlap of molecular orbitals on adjacent molecules. However, in a neutral form, the fractional oxidation state is not present. In order to obtain greater electrical conductivity, the polymer must be oxidized or reduced. The neutral polymer can be chemically converted into an ionic compound consisting of a polymeric cation (for the oxidation case) and a counter-ion which is the reduced form of the oxidizing agent. Similar results can be obtained by utilizing a reducing agent which forms a polymeric anion. The wide use of π-bonded unsaturated polymers for the preparation of conducting polymers is due to the stability of the cation or anion forms of these compounds.[1c] The removal or addition of π electrons does not affect the bonds (sigma) which are responsible for holding

the polymer together. Mild oxidizing or reducing agents such as halogens, sodium napthalide, and quinones are utilized to ensure that only charge-transfer takes place and that no further chemistry occurs. The dopant or counterion perturbs the polymer structure extensively due to its large relative size, and the extensive charge transfer which takes place between the polymer chain and dopant.[6] The range of band-filling obtained utilizing chemical dopants is usually very limited. The chemically doped polymers are also generally insoluble,[9] which prevents the characterization of their redox behavior directly. Recently, interest in conducting polymers has centered on the electropolymerization of heterocycles (polythiophene, polypyrrole) that do not depend on the oxidation or reduction of the polymer by a chemical agent. The synthesis and doping of these materials is accomplished by using a conventional metallic electrode.[9] The level of doping is no longer dependent on the concentration or oxidative (reductive) strength of the counterion, and the doping level can be more easily varied. Electrochemical doping is also cleaner with less interfering chemical reactions. A major problem associated with electrochemically synthesized polymers, however is their insolubility.[9] Typically these polymers have been studied as thin films on electrodes.[10] Kinetic and thermodynamic data have been obtained from these modified electrodes. However, the redox behavior of these films has been shown to be influenced by film discontinuities and non-uniformities, inseparability of faradaic and capacitive currents, and counterion diffusion through the film.[11] The degree of polymerization of many of these polymers is unknown, making a quantitative description of

their properties difficult. Polymer properties are controlled by many factors, including molecular weight, polydispersity, chain branching, crystallinity, and morphology.[5c] Structural defects in the polymer chain can occur because of the formation of charge carriers, specifically polarons and bipolarons. The efforts to understand the chemistry and physics of these materials have been hampered by the insolubility, limited crystallinity, and non-uniformity of these materials.

The second class of electrically conducting materials are called charge-transfer salts or molecular solids. These materials are formed when charge is transferred between donor and acceptor molecules.[4] The donor and acceptor molecules are usually planar molecules that stack upon one another to form segregated arrays. The formation of a band-type electronic structure occurs due the overlap of molecular orbitals of the molecules in the stack.[4] These separate stacks allow the transferred charge to be easily moved along the separate donor and acceptor stacks. The charge-transfer salts must crystallize in a systematic fashion without defects. The synthesis and properties of these materials are influenced by crystal packing forces, intermolecular interactions, and Van der Waal's forces. Defects or disorders in the crystal can cause metal-insulator phase transitions, causing the electrical conductivity to drop to values associated with insulators.[4a] The partial filling of the band occurs due to charge transfer between the donors and acceptors. The degree of band-filling for molecular solids is solely dependant on the properties of the donor and acceptor molecules. It is difficult to compare systems with various levels of band-filling due to

differences in elemental composition, stoichiometries, crystal structure, and band widths.[4,12a]

Very few studies have been performed on non-traditional electrically conducting materials as a function of band-filling. In systems where chemical dopants have been utilized, the variation in band-filling has been limited due to the lack of a wide range of dopants that can be applied on a single system.[13] In charge transfer salts, the ability to tune or change the amount of band-filling is dependent on finding a acceptor-donor molecular systems that will condense together in an organized framework. Recently, through replacement of a fraction of the donor molecules by a molecule of similar size and shape, variation in the amount of band-filling for a charge transfer salt has been obtained.[12] These neutral molecules ensure that the unit cell does not collapse and that the crystal structure is stabilized. The $[NMP]_{1-X}[Phen]_X[TCNQ]$ charge transfer salt, where NMP=N-methylphenazinium, Phen=phenazine and TCNQ = tetracyanoquinodimethane, was synthesized with different ratios of NMP and Phen. Phenazine, a molecule of similar shape and polarizability to NMP, was substituted for NMP into the charge transfer salt. The degree of band-filling varied from 25 to 50% with different ratios of NMP and Phen (fractional charge per cation, cation=donor, TCNQ=acceptor). This particular experiment was the first reported variation in band-filling for a molecular solid. This study also showed the first direct evidence for solitons (structural defects) in a molecular charge-transfer salt.

Electrochemical doping has recently been applied to vary the amount of band-filling in conducting polymers. Wrighton and Ofer

performed a study on the potential dependence of conductivity of a thiophene polymer, by constructing a transistor made out of polymerized thiophene.[14] Two microelectrodes were connected to the redox active polymer, and a fixed potential difference (drain voltage, V_D) was placed across the electrodes. A third electrode was placed between the two microelectrodes to measure the current as the potential (V_G) of the polymer was changed. A plot of I_D vs. V_G reveals the potential dependance of electrical conductivity for the thiophene polymer. The thiophene polymer has a window of high conductivity approximately 1 volt wide. The thiophene polymer is initially an insulator, becomes highly electrically conductive and with further increase in potential (V_G), becomes an insulator again. The potential (V_G) can then be cycled back to the initial potential similar to a cyclic voltammetry experiment (vide infra). A conductivity vs. potential curve of the polymer was obtained. The conductivity vs. potential (I_D vs. V_G) curves for the oxidation scan and the reduction scan are not identical. The differences in the two curves are attributed to changes in the polymer structure. This particular study showed that electrical conductivity does depend on the oxidation of the material. Unfortunately the band-filling as a function of potential could not be determined from this experimental setup. The study was performed in the solid state, thus it is difficult to determine what the nature of the charge carrier in the thiophene polymer is as a function of potential. The technique utilized by Wrighton and Ofer also did not permit the determination of the exact conductivities as a function of potential. The redox behavior of many electrically conductive polymers[1] have been studied

as films on electrodes. Many of those experiments suffer from the same difficulties encountered in this study. Film discontinuities, structural changes, along with the inability to accurately change and determine the degree of band-filling causes the determination of physical and chemical properties as a function of band-filling to be inaccessible from studies utilizing films on electrodes..

Recently, cofacially joined phthalocyanine polymers have been doped by chemical and electrochemical means.[8,13,15] Phthalocyanine polymers combine characteristics of both molecular charge-transfer salts and conducting polymers.[8] Similar to charge-transfer salts, the large planar phthalocyanine molecules are stacked upon one another, permitting the interaction of molecular orbitals and forming a band-type electronic structure. Similar to conducting polymers, the planar phthalocyanine rings or moieties are held together in a rigid-cofacial orientation thru covalent bonds involving the center atom complexed to the phthalocyanine ring. These macrocyclic metal complexes have been bridged with a variety of ligands. Pyrazine, tetrazine, cyanide, and isothiocyanate groups have all been used to bridge Fe, Ru, Co, and Rh phthalocyanines.[1a,16] Axial O-M-O (O = oxygen, M = central metal atom) covalent bonds have been used to bridge Ge, Si, and Sn phthalocyanines.

Chemical doping of both substituted and unsubstituted Si, Ge, and Sn phthalocyanine polymers has been accomplished by a number of groups with iodine, bromine, and nitrosonium salts.[13a,e] The partial oxidation of the unsubstituted Si and Ge phthalocyanine polymers by I_2 and Br_2 was accomplished by stirring the polymer and the corresponding halogen in benzene for 48 hours. Electrical

conductivity of the unsubstituted phthalocyanine polymer $[PcSiO]_n$, doped with iodine increased from 5.5×10^{-6} ohm^{-1} cm^{-1} to 1.4 ohm^{-1} cm^{-1}. Electrical conductivity for $[PcGeO]_n$ doped with iodine increased from 2.2×10^{-10} ohm^{-1} cm^{-1} to 1.1×10^{-1} ohm^{-1} cm^{-1}. The conductivity of these materials increased as the iodine uptake increased, indicating that at higher partial oxidation of the polymer, the number of charge carriers increased. Peripherally substituted Si and Ge phthalocyanines have also been doped in the solid state by halogens.[17] Peripheral substitution with t-butyl groups enables these compounds to be soluble in a number of nonaqueous solvents. Prior to doping, the electrical conductivities of the substituted and unsubstituted polymers were very similar. The highest electrical conductivities for the iodine doped substituted silicon phthalocyanine polymer $[(t\text{-}Bu_4PcSiO)I_Y]_n$ was 2×10^{-3} ohm^{-1} cm^{-1}, and the substituted germanium phthalocyanine polymer $[(t\text{-}Bu_4PcGeO)I_Y]_n$ was 1×10^{-3} ohm^{-1} cm^{-1}. These values are slightly lower than the unsubstituted phthalocyanine polymers. The EPR spectra of the halogen doped substituted silicon polymer shows an intense signal for a free electron, which supports a ligand centered oxidation process. Information obtained from the chemical doping of solid samples does not contain a great deal of information on the band-filling of these compounds. These experiments require long doping times to partially oxidize the polymer. Thus, information on the time dependence of the doping process is lost. With chemical doping, variation in the amount of band-filling by a single dopant is possible by increasing or decreasing the amount of dopant. However, it is not possible to chemically oxidize a polymer from 0 to 100%

homogeneously with a single dopant. Information on the interactive nature of these systems is difficult to probe and usually is not obtainable from studies performed in the solid state.

To obtain a greater control over the amount of band filling, Hanack and Leverenz utilized electrochemical doping in the solid state for the oxidation of μ-pyrazine(phthalocyaninato)iron(II).[18] The potential of the electrode can be used to vary the amount of band-filling. This particular polymer was doped galvanostatically as a weakly pressed pellet in CH_2Cl_2. Galvanostatic doping utilizes a constant current source, the potential of the working electrode varies to keep the same amount of current flowing at all times. Upon galvostatically doping, the electrical conductivity of this polymer increased from 2×10^{-6} ohm^{-1} cm^{-1} to 4.7×10^{-2} ohm^{-1} cm^{-1}. The difficulty with galvostatic doping in the solid state is the inability to separate the faradaic and background currents. Also little information on the rate of electron transfer is obtained from these experiments. However, the power and utility of electrochemical doping is shown by the possibility of tuning the amount of band-filling for a conductive polymer. The greatest electrical conductivity occurred after approximately 50% oxidation of the polymer. At 100% oxidation, the electrical conductivity was 3×10^{-2} ohm^{-1} cm^{-1}, only slightly lower for the value obtained at 50 % oxidation. Theory predicts that this value should be much lower due to the energy expense of pairing mobile charge carriers in the band.[7b] This points out one of the major problem associated with galvanostatic doping in the solid state. The calculation of accurate values of band-filling is difficult, if not impossible. This percent

oxidation is probably less than 100% due to the background current that cannot be subtracted. The insolubility also does not permit the interaction between states to be probed either.

Electrochemical doping of the unsubstituted silicon phthalocyanine polymers has been performed by Marks and co-workers.[15] The silicon polymer was doped as a slurry in a three compartment electrochemical cell. Prior to oxidation, the crystal structure of the silicon polymer was orthorombic. After initial partial oxidation to 50% at E_{app} > +1.80 V and reduction back to the neutral polymer at -0.20 V, the crystal structure of the polymer had changed to a tetragonal phase. The tetragonal phase could then be partially oxidized to 50% at a potential of E_{app} = +1.35 V. The oxidation of the tetragonal phase requires far less energy than the original orthorombic phase. For these slurry doping experiments, the maximum extent of partial oxidation obtainable is dependent on the supporting electrolyte used for the experiment. Different counterions provided different ranges of band filling, the highest partial oxidation, 67% was obtained with the p-toluenesulfonate (TOS^-) counterion.[15d] The electrochemical slurry doping of the unsubstituted silicon phthalocyanines once in the tetragonal phase could be cycled from 0% to 50% and back to 0% oxidation (BF_4^- counterion) without change in redox behavior. The potential range required to go from 0 to 50% oxidation (BF_4^- counterion) began at +0.30 V and ends at +1.20 V. The doping profile of the polymer occurs smoothly and linearly over a 0.90 V range. The undoping of the 50% (BF_4^- counterion) oxidized material again proceeds smoothly and linearly over a 1.0 V range beginning at +0.90 V and ending at -0.10 V. The smoothness of the

doping profiles suggests that there are no additional structural changes accompanying the oxidation process once the polymer is in the tetragonal phase. Optical reflectance data for these materials indicates that at low doping levels (less than 20% oxidation) the phthalocyanine acts as a p-type (radical cation) semiconductor. At slightly higher doping levels the phthalocyanine polymer undergoes an insulator to metal transition and begins to act like a low-dimensional molecular metal. Again these materials are doped in the solid state, prohibiting the acquisition of information on the interaction between redox sites as well as the initial charge transfer event.

The electrochemistry of several various length unsubstituted phthalocyanines oligomers has been reported.[19] The monomer thru tetramer (1 to 4 phthalocyanine rings) materials were capped using t-butyl-dimethylchlorosilane to increase the compound's solubility in nonaqueous solvents. The cyclic voltammograms of these compounds were obtained and compared. For the oligomers, the first oxidation and reduction process is energetically easier (less positive and negative respectively), as the number of phthalocyanine rings increases. In addition, as the oligomer length increases, the potential difference between successive oxidations becomes smaller. This is consistent with decreasing electrostatic repulsion due to delocalization of the charge over a larger aggregate. From the previous studies involving chemical[13] and electrochemical doping[15] of unsubstituted phthalocyanines, it is known that these materials have a band-type electronic structure. Even with these small oligomers, the interaction between adjacent macrocycles can be observed. In

solution, it appears that the cofacially joined phthalocyanines polymers retain their rigid rod cofacial arrangement.

Most doping experiments in the solid state have concentrated only on determining the degree of partial oxidation for a particular doped system. Very little information has been obtained on the chemistry and physics of polymers with interactive redox sites. Solid state doping does not provide detailed information on the charge transfer event or on the rate of charge-transfer between the dopant and conducting polymer. The synthesis of electrically conductive materials that are soluble in conventional solvents is currently an area of considerable interest.[20] The solubility of these systems would allow for the direct characterization of their redox properties by standard electrochemical methodology, eliminating many of the problems associated with solid state doping. Kinetic information on the doping event (i.e. how fast the material can shuttle charge) is an important consideration for many of the future applications of these materials. The substituted phthalocyanine polymers provide an excellent system to study the redox properties of a system with a large amount of interaction between adjacent molecules. From the studies previously performed on substituted and unsubstituted phthalocyanine polymers, it is known that in the solid state, these material possess a band-type electronic structure. The electrochemical studies of the various length oligomers indicate that these materials do interact in solution as shown by the decrease in potential required to oxidize successively larger oligomers. Increases in electrical conductivity (substituted and unsubstituted phthalocyanine polymers) of several orders of magnitude have been

obtained thru the use of chemical or electrochemical (as slurries) doping. Information on the doping process is lost due to the inability to probe the unsubstituted materials. The possibility exists with a soluble conductive polymer, that kinetic information on the rate of electron transfer can be obtained. The solubility of these substituted phthalocyanine polymers could also provide information on the interaction of molecules in a conductive system.

2. Experimental

2.1 Instrumentation

2.1.1 Electrochemical

A Princeton Applied Research (PAR, Princeton, NJ) Model 273 potentiostat / galvanostat, interfaced to a Zenith (Franklin Park, IL) Model 248 AT computer with a National Instruments model PC2A IEEE-488 card for instrument control and data acquisition, was used for the bulk electrolysis and voltammetry experiments. Experimental results were plotted on a Hewlett-Packard (Palo Alto, CA) 7475A plotter. A Bioanalytical Systems (BAS Inc., W. Lafayette, IN) Model 100A potentiostat, interfaced to a Hewlett-Packard Colorpro plotter, was utilized for voltammetry experiments. A Zenith Model 158 XT computer was used to store the acquired data. Inert atmosphere electrochemical studies were performed either in specially designed cells (described in section 2.2.2) or inside a Vacuum Atmospheres (Hawthorne, CA) drybox.

2.1.2 Rotating Electrode Assembly and Bipotentiostat

A Pine Instruments (Grove City, PA) Model AFRDE4 bipotentiostat coupled with a Pine Instruments AFMSR rotator were used to obtain rotating disk voltammograms. The rotation rate for each voltammogram was set by manually adjusting a rpm rate knob on the AFSMR rotator. A Pine Instruments platinum disk and platinum ring-disk electrode were used to obtain the rotating disk voltammograms. A Soltec (San

Fernando, CA) X-Y (Model VP-6423S) or a Soltec X-Y_1-Y_2 (Model VP-6424S) recorder was used to record the voltammograms.

2.1.3 Spectroscopic Instrumentation

UV/Vis spectroscopy were performed with a Beckman (Fullerton, CA) DU-64 spectrophtometer. Spectra were obtained using 1 cm matched quartz cells. ^{1}H NMR spectra were obtained with a Bruker (Billerca, MA) WM-250 250 MHz NMR. All of the ^{1}H spectra are referenced to tetramethylsilane. Fourier transform infrared spectra were obtained on either a Nicolet (Madison, WI) 5-DX or Nicolet 760 instrument. All spectra were obtained as nujol mulls using KBr plates.

2.2 Glassware

2.2.1 Vacuum Lines

All solvents used in the electrochemical experiments were transferred directly into the electrochemical cells using a high vacuum (10^{-5} torr) dual-manifold vacuum line. After solvent transfer, the electrochemical cells were backfilled with argon (Matheson, 99.95%) to ensure their anaerobic integrity. The argon had been passed through a drying column (Mn on silica) to remove residual oxygen and moisture. Synthetic steps requiring the exclusion of either air or moisture, were performed using standard Schlenk-line techniques.[21]

2.2.2 Electrochemical Cells

Several types of electrochemical cells that interface directly to the high vacuum line thru ground glass joints were used in these studies. Controlled potential coulometry was carried out in an all glass three compartment cell.[22] The counter electrode, constructed

of Pt gauze, was isolated from the working electrode compartment by two fine porosity glass frits. The reference electrode, a Ag wire, was separated from the working cell compartment by a fine porosity glass frit. The working electrode for bulk coulometry studies was constructed from Pt gauze and was approximately 8 cm^2 in area. A small area (0.018 cm^2) platinum disk working electrode (BAS Inc., W. Lafayette, IN) was also placed in the working compartment of the cell to allow voltammetry studies to be performed. The small area Pt working electrode was polished with 0.05 μm alumina (Buehler, Lake Bluff, IL) prior to use.

Experiments involving only voltammetric measurements (cyclic voltammetry, differential pulse voltammetry) were performed in single compartment cells that also interfaced to a high vacuum line thru a ground glass joint. A small area (0.018 cm^2) platinum disk electrode (BAS Inc., W. Lafayette, IN), a platinum wire counter electrode, and a Ag wire reference electrode were used in these cells.

Rotating voltammetry experiments were performed in a three compartment cell specially designed to reduce the formation of a vortex.[23] A Ag wire reference electrode and a Pt gauze counter electrode were placed in sidearm compartments separated from the main part of the cell by fine porosity glass frits. A Pt ring-disk (Pine

Instruments, Grove City, PA) or a Pt disk electrode was used as the working electrode (area of disk = 0.163 cm^2).

2.3 Chemicals

2.3.1 Synthesis Solvents

Pyridine was dried and purified by distillation from CaH_2 under N_2. Quinoline was stirred over barium oxide for two days and then decanted. The decanted quinoline was then vacuum distilled and stored over activated 3Å sieves. Methanol was dried by distilling from magnesium under N_2. Ether was dried and deaerated by distilling from sodium/benzophenone under N_2. Chloroform was dried and purified by distillation from CaH_2 under N_2.

2.3.2 Electrochemical Solvents

1,1,2,2-tetrachloroethane (Aldrich Chemical, Milwaukee, WI) was stirred with CaH_2 for 48 hours, then vacuum distilled. The resulting solvent was degassed by six freeze-pump-thaw cycles (liquid N_2) on a high vacuum line, and then vacuum transferred to a specially designed round bottom solvent bulb containing activated 3Å molecular sieves. For storage the solvent was subsequently freeze-pump-thaw one additional time to ensure deaeration.

Tetrahydrofuran (HPLC grade, Burdick and Jackson, Muskegon MI) was dried by addition of sodium-potassium amalgam (NaK). It was degassed by six cycles of a freeze-pump-thaw sequence.

Methylene chloride (HPLC grade, Burdick and Jackson, Muskegon MI.) was degassed by four cycles of a freeze-pump-thaw sequence, and then dried by stirring for three days with activated 3Å sieves. The

dried solvent was then transferred to a solvent bulb containing activated 3Å sieves and treated to a final freeze-pump-thaw cycle.

2.3.3 Supporting Electrolyte

Tetrabutylammonium fluoroborate ($TBABF_4$, electrometric grade, Southwestern Analytical Chemicals, Austin, TX) was recrystallized from ethyl acetate/diethyl ether and dried under dynamic vacuum (10^{-5} torr) for 2 days.

2.4 Synthesis

2.4.1 Trans-dichloro(tetra-t-butylphthalocyaninato)silicon

The μ-oxo-(tetra-t-butylphthalocyaninato)silicon polymer $(t\text{-}Bu_4PcSiO)_n$ (Figure 2) was prepared by a modification of the literature procedure.[17a,c] The synthesis of the polymer requires 10 steps from the initial starting materials. The individual steps are outlined in Scheme 1. Several problems were encountered in the synthesis of the dichloro(tetra-t-butylphthalocyaninato)silicon $t\text{-}Bu_4PcSiCl_2$ (step 8 in Scheme 1). Following the literature procedure for the synthesis of $t\text{-}Bu_4PcSiCl_2$ (8), 5-t-butyl-1,3-diiminoisoindoline (5 g, 25 mmol, 95% pure by NMR) and 4.1 mL of $SiCl_4$ (Aldrich Chemical Co., Milwaukee, WI) were refluxed for 30 minutes in dry quinoline under argon. The reaction mixture turned dark green and, after allowing it to cool to room temperature, was diluted with 400 mL of dry chloroform. HCl gas (Matheson, Lynhurst, NJ) was bubbled through this solution for 1 hour. It was then filtered to remove any insoluble material (none was present). The filtrate was reduced in volume under vacuum to the point where

Figure 2. Schematic of the peripherally substituted phthalocyanine polymer $(t\text{-}Bu_4PcSiO)_n$, central metal atom = Si, the chain length of this polymer is approximately 25 units.[17b]

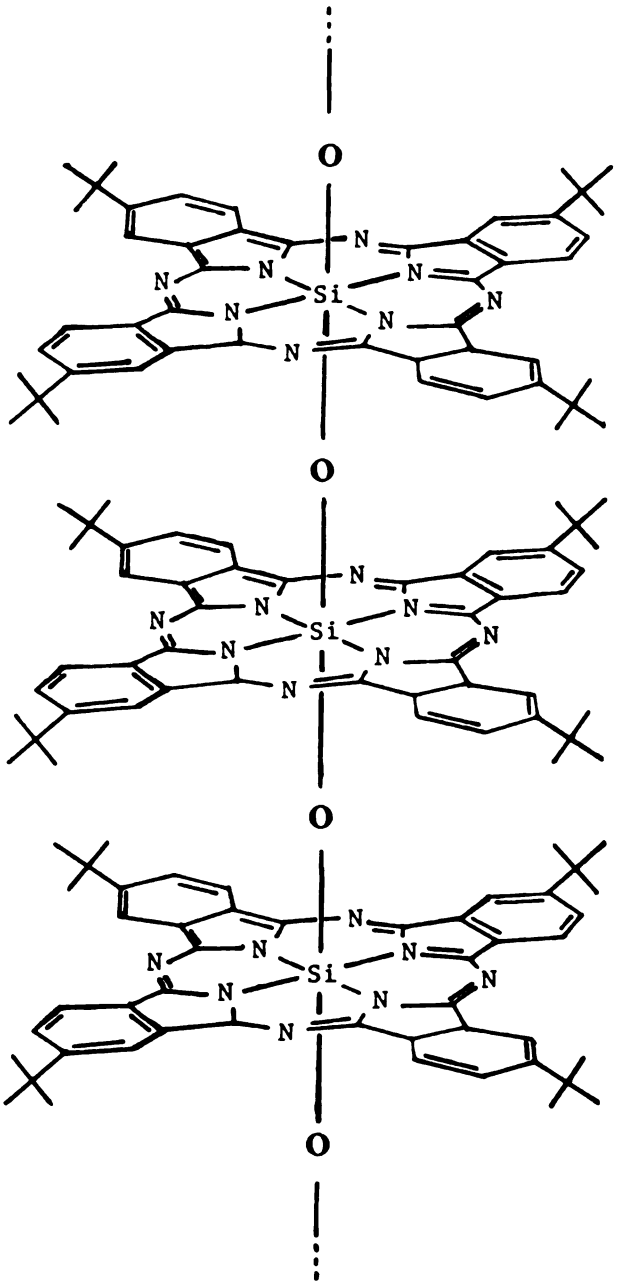

FIGURE 2

SCHEME 1

SYNTHESIS OF $(t\text{-}Bu_4PcSiO)_n$

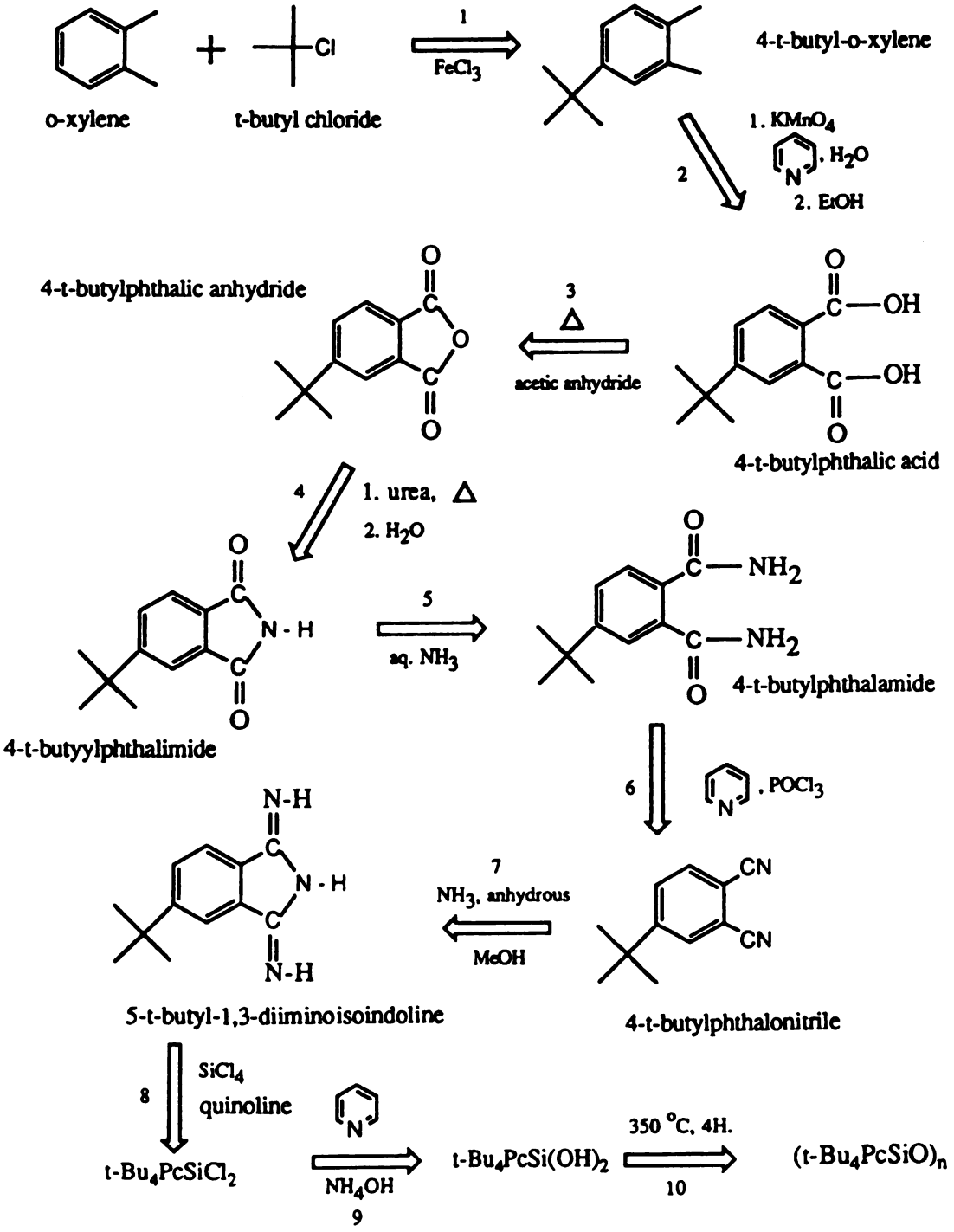

crystallization began. The resulting thick green solution was filtered under argon with great difficulty resulting in the isolation of a small amount (0.1 g) of a microcrystalline powder. The reported ^1H NMR spectrum ($CDCl_3$) for t-$Bu_4PcSiCl_2$ (8) has peaks at δ1.8 ppm (CH_3 of the t-butyl group) and multiplets at 8.4 and 9.5 (ring protons on the phthalocyanine).[17c] The ^1H NMR spectrum ($CDCl_3$) of the isolated material showed a series of peaks in the δ1.0 to 2.0 ppm region, (large singlet at 1.6 ppm, small singlet at 1.8 ppm). Other peaks were observed at 7.9-8.1 ppm (multiplet), and 8.9-9.0 ppm (multiplet), no peaks were observed at either 8.4 or 9.5 ppm. The synthesis of was repeated four more times with similar results.

The ^1H NMR spectra and correspondence with Professor M. Hanack of the Univ. of Tubigen FRG, suggested that the product of the above reactions was a quinoline adduct of the desired compound. Upon his advice, the experimental procedure was modified in an attempt to destroy this adduct. After refluxing 5-t-butyl-1,3-diiminoisoindoline (5 g, 25 mmol, 95% pure by NMR) and 4.1 mL of $SiCl_4$ for 30 minutes in quinoline, the solution was allowed to cool to room temperature. To this solution 400 mL of concentrated HCl was added. The resulting mixture was then heated to 50 ^oC and gently stirred for one hour. The reaction mixture was then suction filtered in air and washed with copious amounts of HCl and water. The ^1H NMR spectrum of the resulting product indicated that the desired product was formed and was approximately 90% pure. The t-$Bu_4PcSiCl_2$ (8) being slightly soluble in ether, was purified via soxlet extraction. The ^1H NMR spectra of the ether extracted material (Figure 3) was

Figure 3. ^{1}H NMR spectrum of dichloro(tetra-t-butylphthalocyaninato)silicon, t-$Bu_4PcSiCl_2$, obtained in $CDCl_3$. The spectrum is referenced to tetramethylsilane and the peak at 7.24 ppm is due to residual $CHCl_3$. Peak assignments are given in the text.

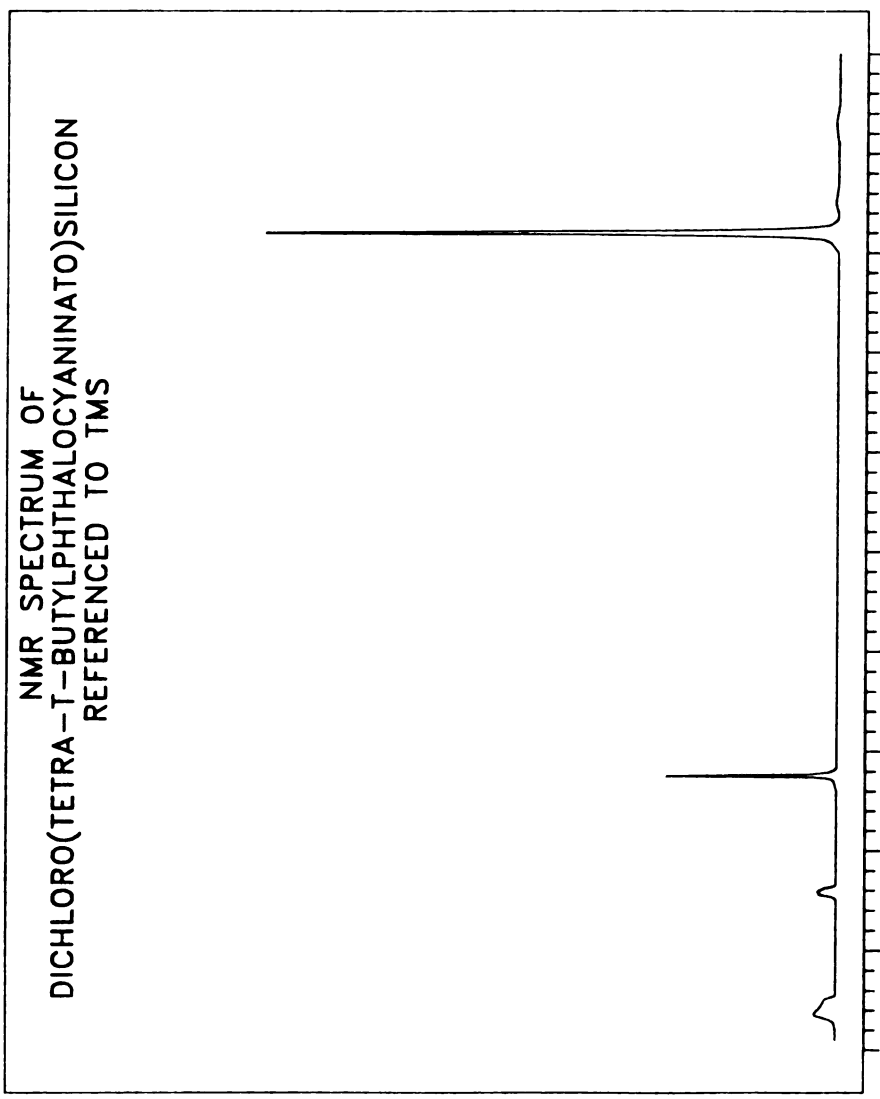
NMR SPECTRUM OF
DICHLORO(TETRA-T-BUTYLPHTHALOCYANINATO)SILICON
REFERENCED TO TMS
10.0
9.0
8.0
7.0
6.0
5.0
4.0
3.0
2.0
1.0
0.0
PPM

FIGURE 3

identical to that reported in the literature and was approximately 98% pure.

2.4.2 Dihydroxy(tetra-t-butylphthalocyaninato)silicon

The procedure for the conversion of [t-Bu_4PcSi$(Cl)_2$] (8) to dihydroxy(tetra-t-butylphthalocyaninato)silicon [t-Bu_4PcSi$(OH)_2$] (9) involved a slight modification of the literature method.[17c] A suspension of t-Bu_4PcSiCl_2 was heated to 60 °C in 50 mL of a 50/50 mixture of ammonium hydroxide/pyridine in a sealed pressure tube for 24 hours. The resulting material was isolated by suction filtration and dried under vacuum (10^{-3} torr). UV/Vis (Figure 4) and FTIR (Figure 5) spectra of the dihydroxy capped monomer, t-bu_4PcSi$(OH)_2$, closely match those reported in the literature.[17a] The large absorbance peaks occur at 679 and 354 nm. The reported literature values are 680 and 350 nm.[17a]

2.4.3 μ-oxo-(tetra-t-butylphthalocyaninato)silicon

The μ-oxo-(tetra-t-butylphthalocyaninato)silicon polymer (10) was formed by heating [t-Bu_4PcSi$(OH)_2$] to 350 °C under dynamic vacuum (10^{-5} torr) for 4 hours, in a tube furnace (Lindberg, Watertown, WI).[17a] UV/Vis (Figure 6) and FTIR (Figure 7) spectra of the silicon polymer, (t-bu_4PcSiO)$_n$, closely match those reported in the literature.[17a] The degree of polymerization of the silicon polymer

Figure 4. UV/Vis spectrum of dihydroxy(tetra-t-butylphthalocyaninato)silicon, t-$Bu_4PcSi(OH)_2$, obtained in CH_2Cl_2. Absorbance peaks occur at 679 and 354 nm.

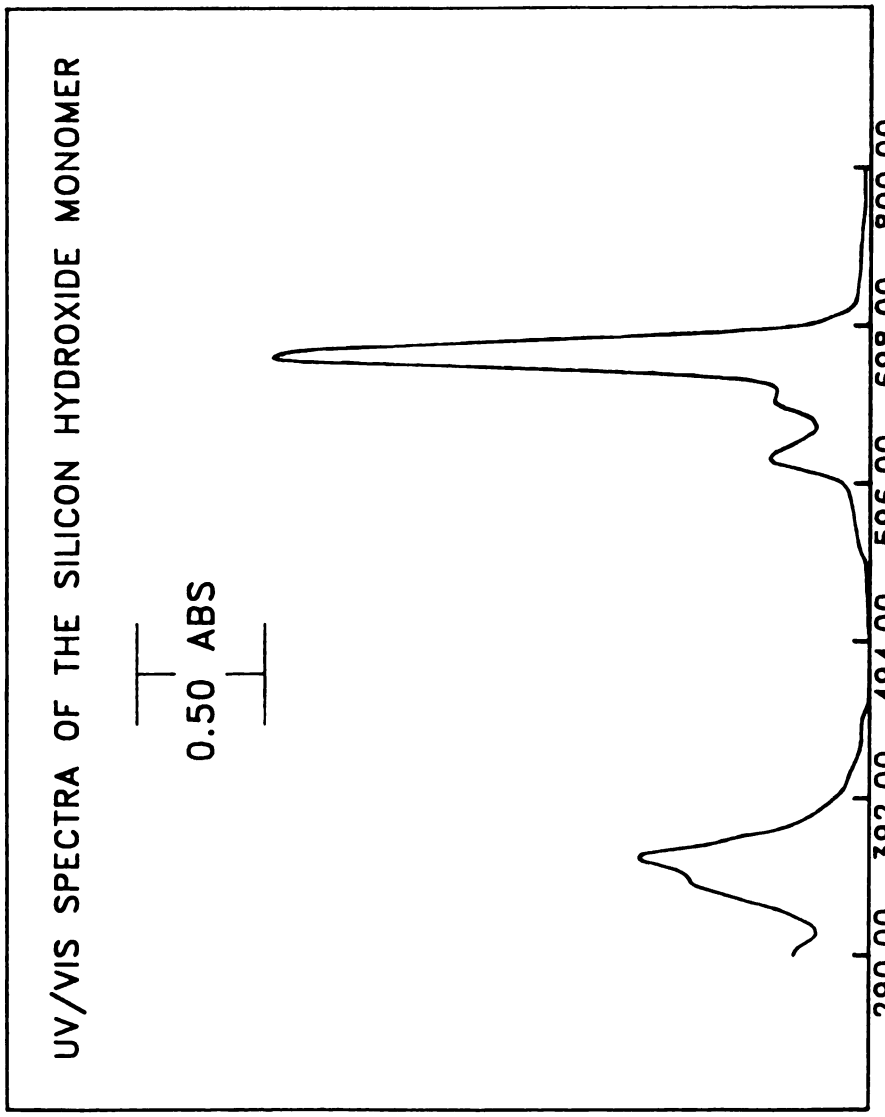
UV/VIS SPECTRA OF THE SILICON HYDROXIDE MONOMER
0.50 ABS
290.00
392.00
494.00
596.00
698.00
800.00
WAVELENGTH (NM)

FIGURE 4

Figure 5. FT-IR spectrum of dihydroxy(tetra-t-butylphthalocyaninato)silicon, t-$Bu_4PcSi(OH)_2$, obtained as a nujol mull. The IR spectrum is identical to that reported in the literature including the OH stretching vibration at 3500 cm^{-1}.

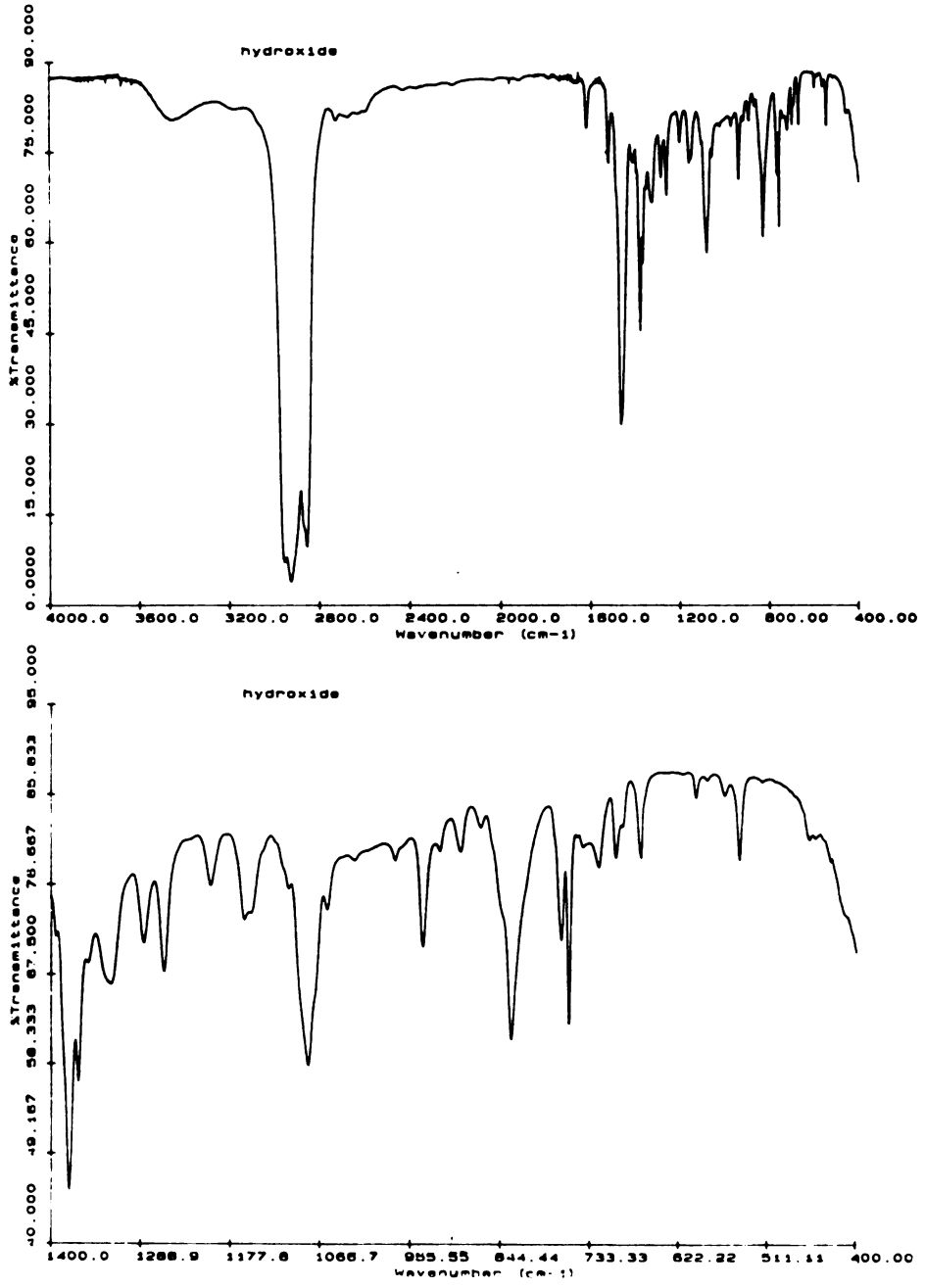
hydroxide
%Transmittance
90.000
75.000
60.000
45.000
30.000
15.000
0.0000
4000.0
3600.0
3200.0
2800.0
2400.0
2000.0
1600.0
1200.0
800.00
400.00
Wavenumber (cm-1)
hydroxide
%Transmittance
95.000
85.833
76.667
67.500
58.333
49.167
40.000
1400.0
1288.9
1177.8
1066.7
955.55
844.44
733.33
622.22
511.11
400.00

FIGURE 5

Figure 6. UV/Vis spectra of the pristine, unoxidized silicon polymer, $(t\text{-}Bu_4PcSiO)_n$, obtained in CH_2Cl_2. The absorbance peaks occur at 619 and 327 nm.

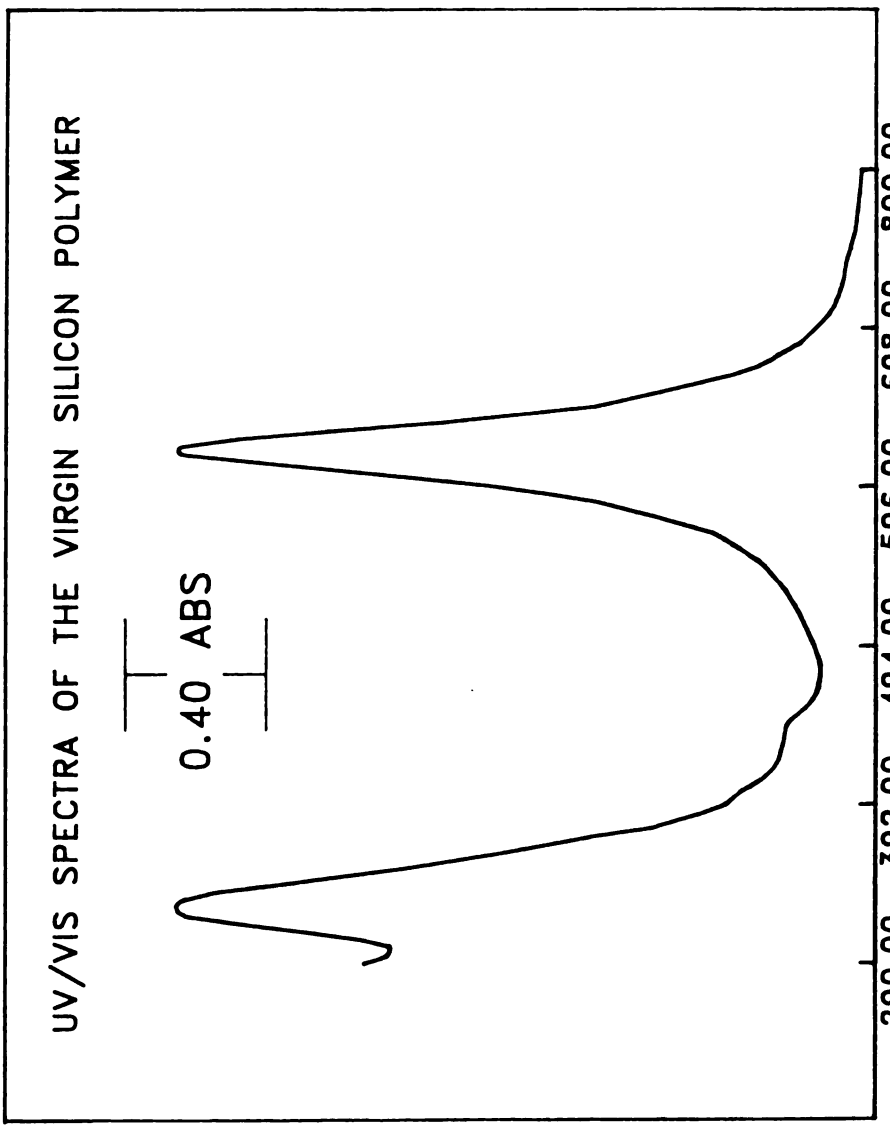
UV/VIS SPECTRA OF THE VIRGIN SILICON POLYMER
0.40 ABS
290.00
392.00
494.00
596.00
698.00
800.00
WAVELENGTH (NM)

FIGURE 6

Figure 7. FT-IR spectrum of μ-oxo(tetra-t-butylphthalocyaninato)silicon $(t\text{-}Bu_4PcSiO)_n$, obtained as a nujol mull. The IR spectrum is identical to that reported in the literature.

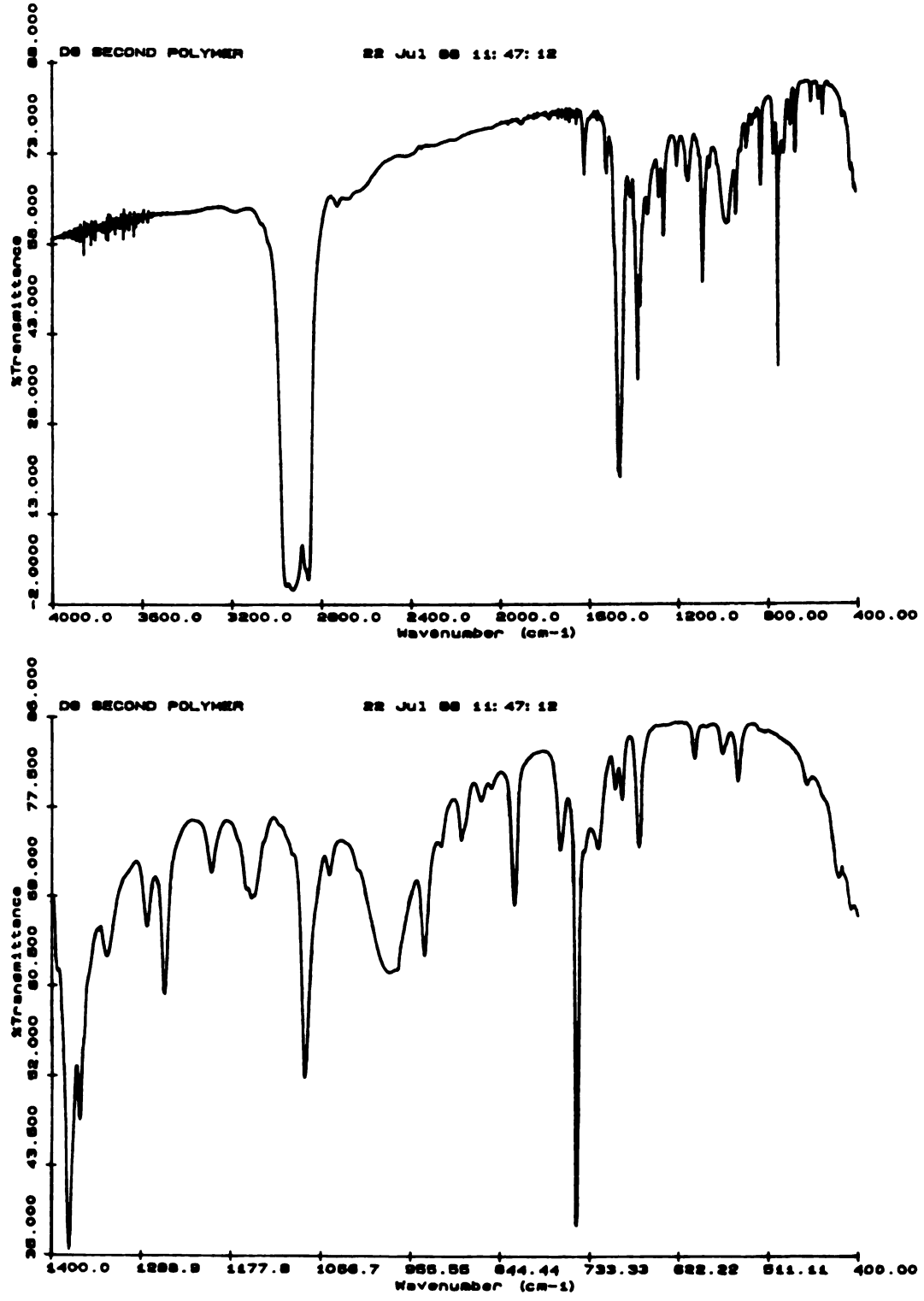
D8 SECOND POLYMER
22 Jul 88 11:47:12
%Transmittance
98.000
73.000
48.000
23.000
-2.0000
4000.0
3600.0
3200.0
2800.0
2400.0
2000.0
1600.0
1200.0
800.00
400.00
Wavenumber (cm-1)
D8 SECOND POLYMER
22 Jul 88 11:47:12
%Transmittance
86.000
77.500
69.000
60.500
52.000
43.500
35.000
1400.0
1288.9
1177.8
1066.7
955.55
844.44
733.33
622.22
511.11
400.00
Wavenumber (cm-1)

FIGURE 7

$(t\text{-}bu_4PcSiO)_n$, has been determined by Hanack and coworkers by end-group analysis to be 25.[17b]

2.4.4 Bis(trimethylsiloxy)(tetra-t-butylphthalocyaninato)silicon

Bis(trimethylsiloxy)(tetra-t-butylphthalocyaninato)silicon $(t\text{-}Bu_4PcSiO_2)(Si(CH_3)_3)_2$, the capped monomer, was obtained by refluxing 1.0 mL of trimethylchlorosilane (Fluka Chemie AG, Ronkonkoma, NY), 0.10 grams of dried $t\text{-}Bu_4PcSi(OH)_2$, and 20 mL of pyridine for five hours. The resulting solution was taken to dryness and the excess silane was removed in vacuo (10^{-3} torr). The dried solids were chromatographed on alumina (activity 1) using toluene-hexane (1:2) as the eluant. The capped monomer was the first major visible band. Several indistinct bands came off after main band of capped monomer. These bands may have been higher oligomers, however their limited concentration prevented characterization. The ^1H NMR of the capped monomer in $CDCl_3$ (Figure 8) was δ9.55 (m, 3,6-Pc), 8.39 (m, 5-Pc), 1.81 (s, t-bu), -2.78 (s, CH_3).

Figure 8. ^{1}H NMR spectrum of bis(trimethylsiloxy)(tetra-t-butylphthalocyaninato)silicon, (t-Bu_4PcSiO_2)($Si(CH_3)_3)_2$, obtained in $CDCl_3$. The spectrum is referenced to tetramethylsilane and the peak at 7.24 ppm is due to residual $CHCl_3$. Peak assignments are given in the text.

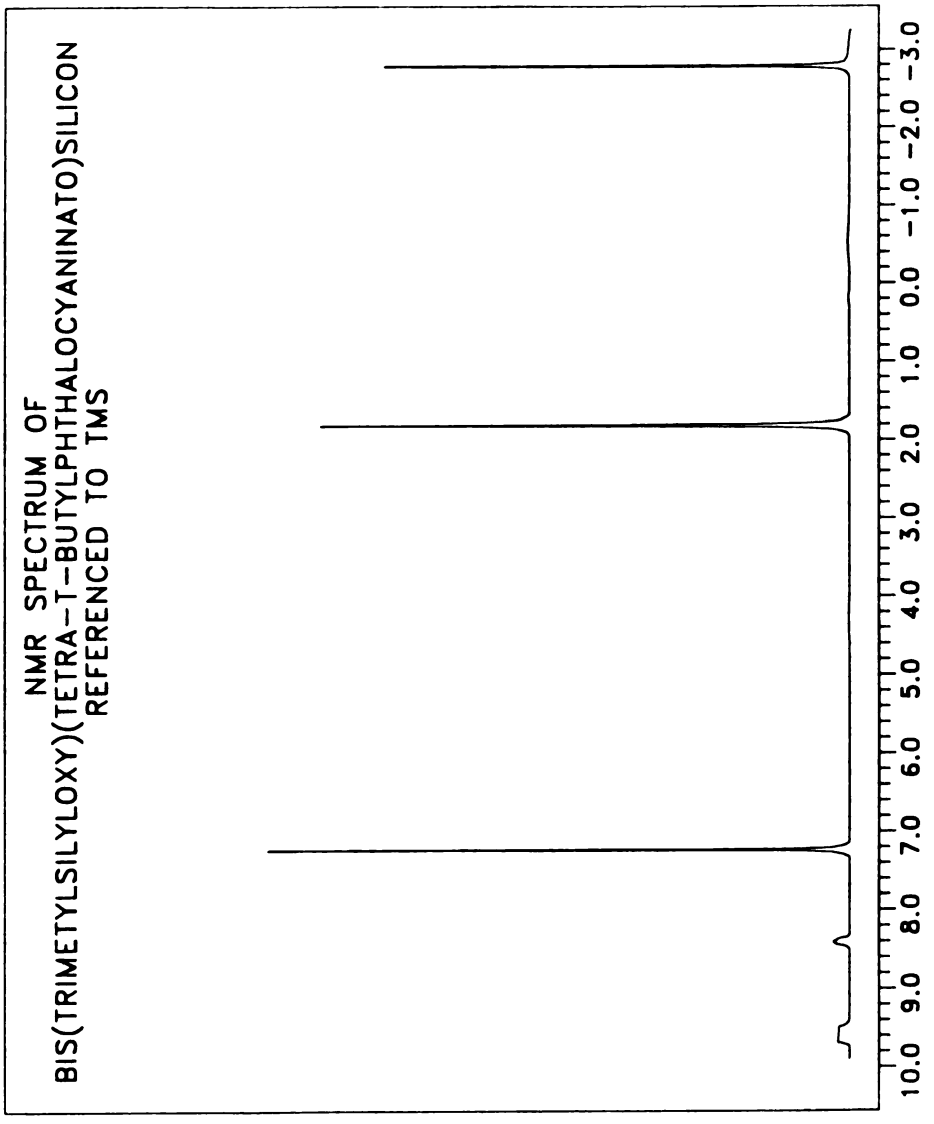
NMR SPECTRUM OF
BIS(TRIMETYLSILYLOXY)(TETRA-T-BUTYLPHTHALOCYANINATO)SILICON
REFERENCED TO TMS
10.0 9.0 8.0 7.0 6.0 5.0 4.0 3.0 2.0 1.0 0.0 -1.0 -2.0 -3.0
PPM

FIGURE 8

3. Electrochemical Studies of μ-oxo-(tetra-t-butylphthalocyaninato)silicon

3.1 Bulk Oxidation by Controlled Potential Coulometry

3.1.1 Introduction

Bulk electrolysis is used to convert a compound from one oxidation state to another, and can be used to determine the number of electrons involved in the process.[24] This is usually accomplished by controlling the potential of the working electrode and integrating the resultant current with time (CPC, Controlled Potential Coulometry). Rapid stirring of the solution is used to ensure efficient mass transfer of material to the working electrode. Controlled potential coulometry (CPC) was employed to determine the degree of partial oxidation as a function of potential. This technique was used since it is an absolute electrochemical method for determining oxidation states.[24] All of the polymer in the cell is converted to a specific oxidation state depending on the potential of the working electrode.

3.1.2 Procedure

Supporting electrolyte ($TBABF_4$) was weighed out and added to the three compartments of the CPC cell (Figure 9). The amount of supporting electrolyte ($TBABF_4$) in all three compartments was enough to produce a 0.2 M solution. A known amount of $(t\text{-}Bu_4PcSiO)_n$ polymer (11.0 to 12.0 mg, 0.55 to 0.60 mg/mL) was added to the working compartment of the cell. The coulometry cell was then connected to a high vacuum line and evacuated (10^{-5} torr). After the entire cell

Figure 9. All ground glass joint coulometry cell utilized for the bulk oxidations of the silicon polymer. The counter electrode (Pt mesh, 2 cm^2 in area) is separated from the working electrode by two fine porosity glass frits. The Ag wire reference electrode is separated from the working solution by a fine porosity glass frit. The working electrode is constructed of Pt mesh approximately 8 cm^2 in area. A small area Pt (0.018 cm^2) electrode was also placed into the working solution.

A - ground glass joints, B - counter electrode

C - glass frits, D - working electrode

E - small area working electrode, F - reference electrode

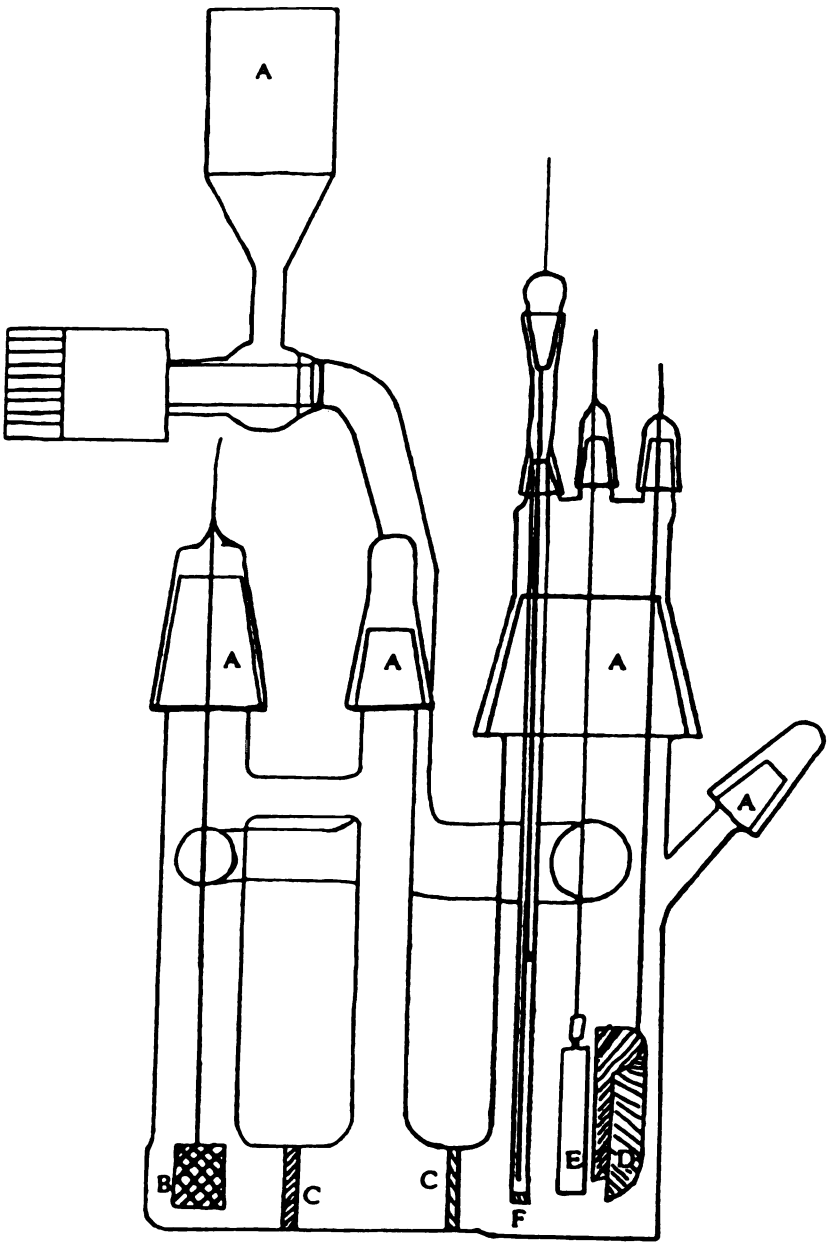

FIGURE 9

was cooled with an isopropanol-dry ice bath, a known amount of solvent was vacuum transferred. The cell was then backfilled with argon to ensure anaerobic conditions. After allowing the solution to warm to room temperature, the cell was ready for use.

3.1.3 Results

The CPC oxidation experiments were conducted on neutral polymer dissolved in 1,1,2,2-tetrachloroethane. The potential for the onset of oxidation of the polymer was determined from rest potentials of the solution and differential pulse voltammetry (DPV) experiments. Before the initial bulk electrolysis experiments were run, it was necessary to ensure that the polymer was in its neutral form.[25] This was accomplished by reducing the initial solution at a potential where the differential pulse voltammetry (DPV, vide infra) response exhibited only background current (the region between the onset of oxidation and reduction). The as-synthesized or virgin material had typically been oxidized a few percent.[25] After this procedure the potential of polymer solution was approximately zero (0) volts.

To "map-out" the % oxidation vs. potential profile for the polymer, a series of CPC experiments were performed. The working electrode potential was set to a value where oxidation of the polymer would occur. The resulting current was monitored as a function of time until it decayed to a limiting background value (Figure 10). Generally, the background current (10^{-7} A/cm^2) was three orders of magnitude less than the initial current (10^{-4} A/cm^2). The number of coulombs passed at a given potential was determined by integrating the current over time. This value is comprised of contributions from both the oxidation of the polymer and any background processes.

Figure 10. Current-time curves for the oxidation of neutral silicon polymer, $(t\text{-}Bu_4PcSiO)_n$, in 1,1,2,2-tetrachloroethane / 0.2 M $TBABF_4$ at different potentials. The solution concentration was 0.0288 mM based on a 25 phthalocyanine unit polymer or 0.72 mM based on a single phthalocyanine moiety.

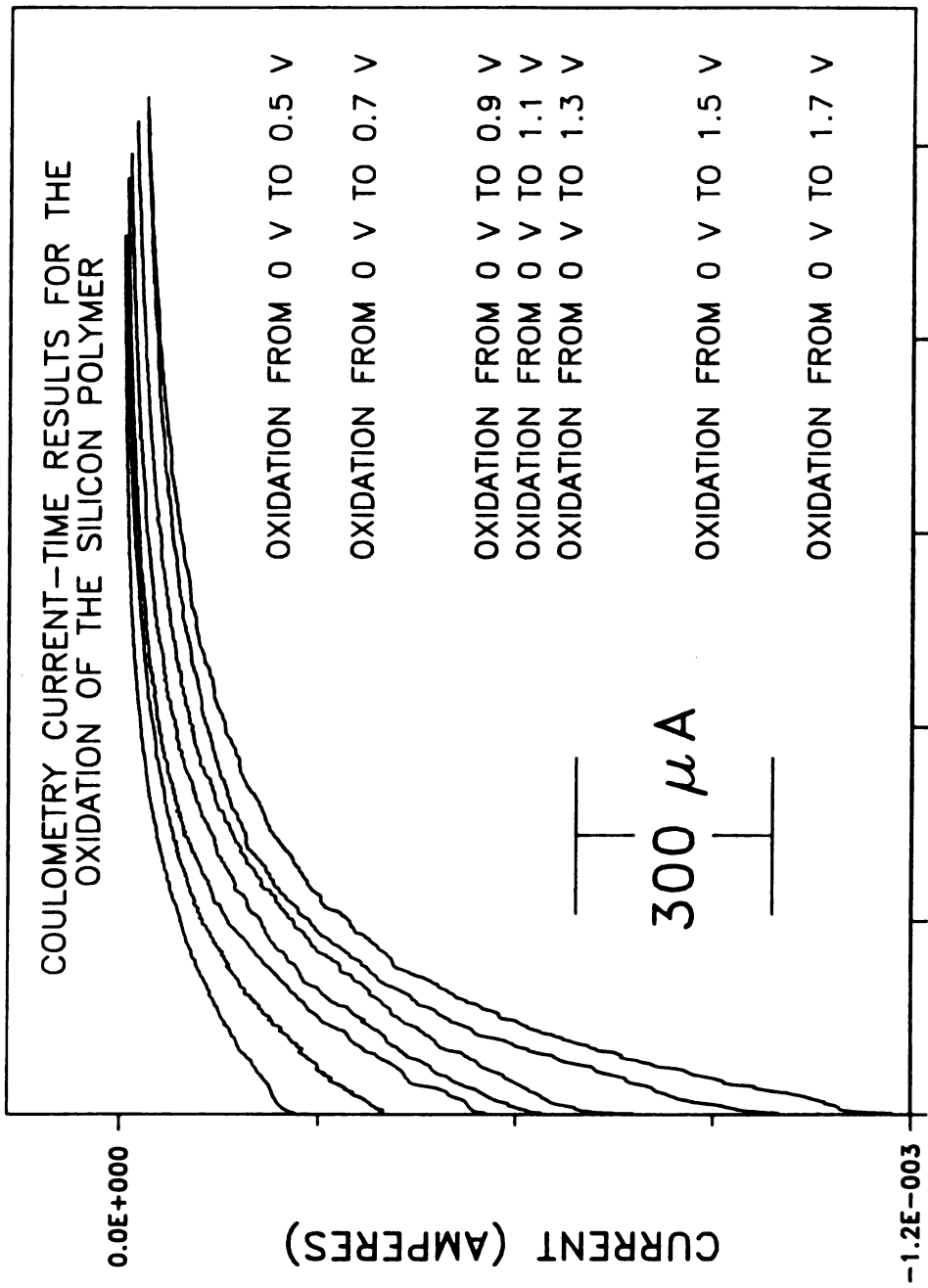
COULOMETRY CURRENT–TIME RESULTS FOR THE OXIDATION OF THE SILICON POLYMER
OXIDATION FROM 0 V TO 0.5 V
OXIDATION FROM 0 V TO 0.7 V
OXIDATION FROM 0 V TO 0.9 V
OXIDATION FROM 0 V TO 1.1 V
OXIDATION FROM 0 V TO 1.3 V
OXIDATION FROM 0 V TO 1.5 V
OXIDATION FROM 0 V TO 1.7 V
300 μA
CURRENT (AMPERES)
0.0E+000
-1.2E-003
0.00
20.00
40.00
60.00
80.00
100.00
TIME (MINUTES)

FIGURE 10

Since the current arising from the background oxidations are usually constant over the lifetime of the experiment, the amount of charge consumed by these events can be estimated by multiplying the total time of the experiment by the limiting background current value. The net number of coulombs for oxidation of the polymer was calculated by subtracting the number of background coulombs from the number of gross coulombs recorded. Once the polymer was oxidized, it was then reduced back to the neutral state (Figure 11) by setting the potential of the working electrode to a value 50 mV negative of the rest potential of the neutral polymer. The stability of the polymer was checked by DPV after this cycle. Once the polymer was back in the neutral form, another oxidation/re-reduction cycle was run at a different potential. In order to map out the % oxidation vs. potential curve (Figure 12), a total of 10 oxidation/re-reduction cycles were run.

The number of electrons transferred for a simple redox process can be calculated from Faraday's law.

$$Q = n F N \qquad (1)$$

where:

Q = charge (coulombs)

n = number of electrons

F = Faraday's constant (96,485 coulombs $mole^{-1}$)

N = moles of analyte

The $(t\text{-}Bu_4PcSiO)_n$ polymer is comprised of redox active sites coupled together thru axial covalent bonds. The number of sites in the

Figure 11. Current-time curves for the reduction of oxidized silicon polymer, $(t\text{-}Bu_4PcSiO)_n$, in 1,1,2,2-tetrachloroethane / 0.2 M $TBABF_4$ at different potentials. The solution concentration was 0.0288 mM based on a 25 phthalocyanine unit polymer or 0.72 mM based on a single phthalocyanine moiety.

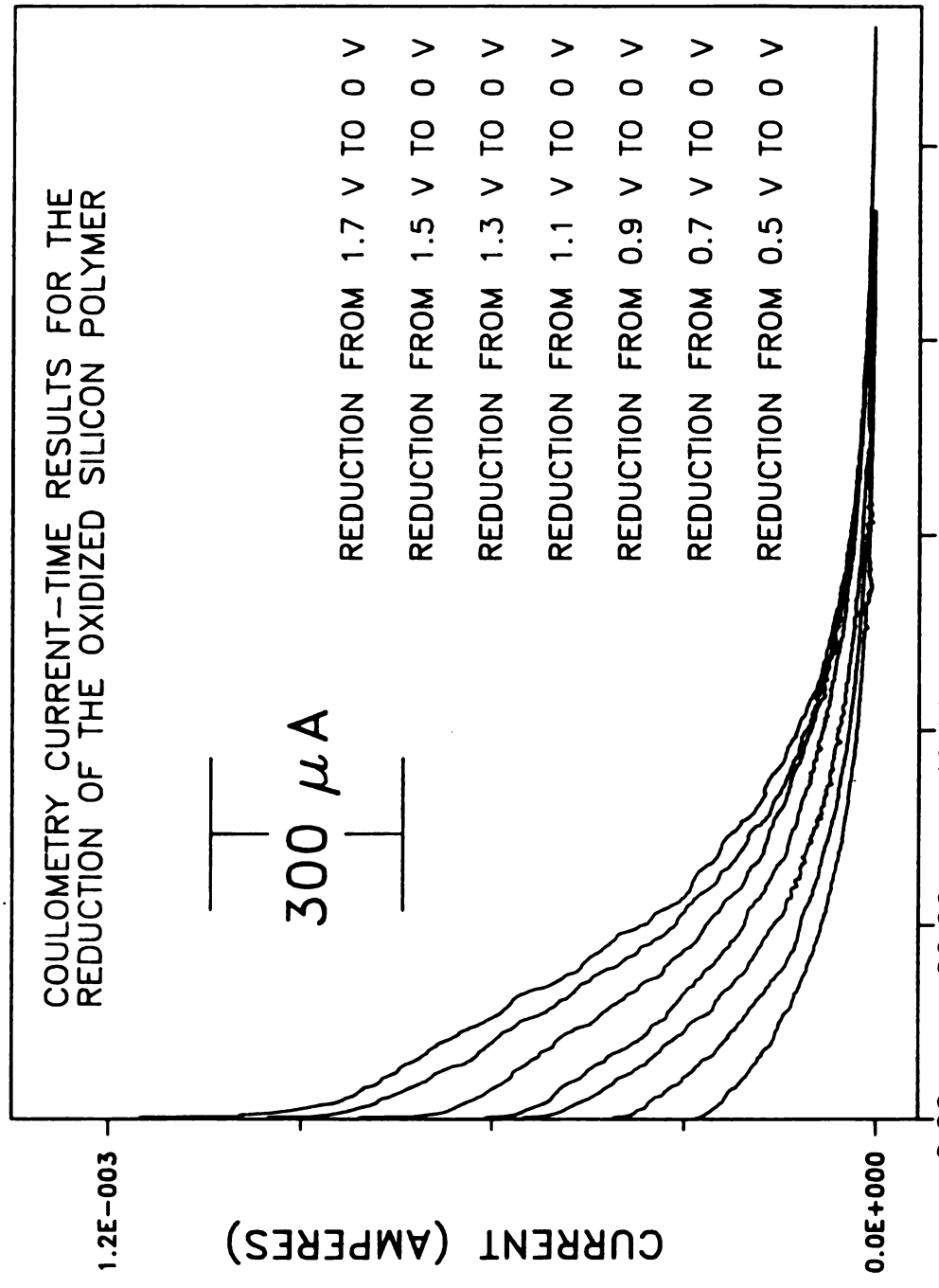
COULOMETRY CURRENT-TIME RESULTS FOR THE
REDUCTION OF THE OXIDIZED SILICON POLYMER
300 μA
REDUCTION FROM 1.7 V TO 0 V
REDUCTION FROM 1.5 V TO 0 V
REDUCTION FROM 1.3 V TO 0 V
REDUCTION FROM 1.1 V TO 0 V
REDUCTION FROM 0.9 V TO 0 V
REDUCTION FROM 0.7 V TO 0 V
REDUCTION FROM 0.5 V TO 0 V
1.2E-003
0.0E+000
CURRENT (AMPERES)
0.00
20.00
40.00
60.00
80.00
100.00
TIME (MINUTES)

FIGURE 11

Figure 12. The degree of oxidation vs. potential for the electrochemical oxidation of the silicon polymer, $(t\text{-}Bu_4PcSiO)_n$, in 1,1,2,2-tetrachloroethane / 0.2 M $TBABF_4$. Each point corresponds to the mean value for a complete oxidation/re-reduction cycle performed by controlled potential coulometry. The error bars represent the difference between the oxidation and re-reduction values. Solutions were typically 0.02 to 0.04 mM based on a 25 phthalocyanine unit polymer or 0.5 to 1 mM, based on a single phthalocyanine moiety (0.4 - 0.8 mg polymer/mL). The % oxidation values were determined by relating the mass of material present to the amount of charge passed at the given potential (see equation 2).

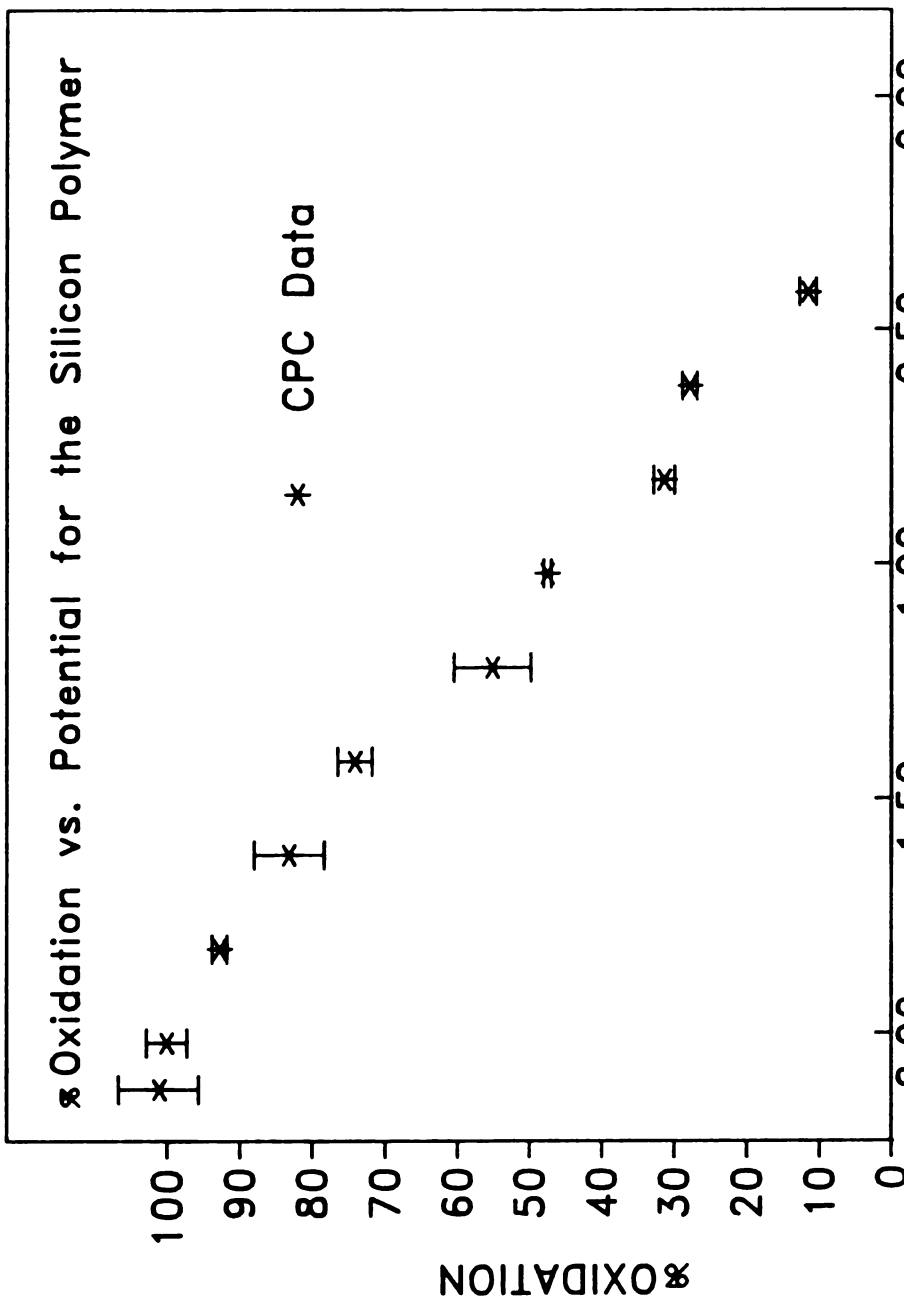
% Oxidation vs. Potential for the Silicon Polymer
CPC Data
% OXIDATION
POTENTIAL (Volts vs. SSCE)
0
10
20
30
40
50
60
70
80
90
100
2.00
1.50
1.00
0.50
0.00

FIGURE 12

polymer depends on the degree of polymerization. Oxidation of neutral polymer causes charge to be removed from these sites. Results of the coulometry experiments are expressed as percent oxidation, or percentage of polymer oxidation. Since each phthalocyanine ring is a site for oxidation, the number of phthalocyanine moieties in each experiment must be calculated. This can be done from the number of grams of polymer used, and the molecular weight (781 grams $mole^{-1}$) of a single phthalocyanine unit.[17a] From the number of moles of -(t-Bu_4PcSiO)- (phthalocyanine moieties), and the number of coulombs passed, the % oxidation of the material can be determined by:

$$Q_{exp} \; (\; WT \; / \; MW * F \;) = n \qquad (2)$$

where:

Q_{exp} = experimentally determined coulombs

WT = weight of $(t\text{-}Bu_4PcSiO)_n$ in grams

MW = molecular weight of -(t-Bu_4PcSiO)-

F = Faraday's constant (96,485 coulombs $mole^{-1}$)

n = fractional number of electrons transferred per site

The % oxidation at a specific potential is determined by ratioing the number of coulombs measured at that potential to those required for 100 % oxidation. These results are summarized in Table 1 and Figure 12. By varying the potential of the working electrode, and calculating the number of background corrected coulombs at the different potentials, the percent oxidation at different potentials was determined. The % oxidation vs. potential profile of the polymer

TABLE 1

% OXIDATION VS. POTENTIAL FOR THE SILICON POLYMER

POTENTIAL[a]	CPC DATA[b]	RDE DATA[c]	SIMULATION DATA[d]
0.42	11.5 (± 1.2)	14.3 (± 0.6)	8.5
0.64	27.9 (± 1.0)	21.2 (± 0.6)	18.9
0.82	31.4 (± 1.5)	30.5 (± 1.0)	30.6
1.02	47.5 (± 0.6)	41.6 (± 1.0)	41.9
1.22	55.1 (± 5.4)	52.7 (± 1.2)	50.7
1.42	74.1 (± 2.4)	68.3 (± 1.5)	65.5
1.62	83.2 (± 4.8)	85.1 (± 2.1)	84.6
1.82	93.0 (± 1.1)	100[e]	99.9
2.02	100.0 (2.8)	100[e]	100.0

[a] potential in volts (V) vs. aq. SSCE in 1,1,2,2-tetrachloroethane.

[b] average value and the deviation based on the inital oxidation of the polymer and rereduction back to the neutral form.

[c] average value and the deviation based on the voltammograms shown in Figure 13. See the text for complete details.

[d] based on 25 redox sites. The standard potentials for each couple used in the simulation are listed in Table II. See the text for complete details.

[e] limiting current of the RDE voltammograms were taken as representing 100% oxidation.

shown in Figure 12 occurs over a 1700 mV range, which is indicative of a polymer in which there is a large degree of interaction between the redox sites. As the error bars illustrate (Figure 12), the number of coulombs necessary for the oxidization and subsequent re-reduction back to neutral $(t\text{-buPcSiO})_n$ polymer were virtually identical . The small difference in these values suggests that the polymer is stable at all degrees of partial oxidation. The smooth doping profile suggests that there is a continuum or band from which charge can be removed and that there is no large amount of inherent stability at any particular degree of partial oxidation. If there was some instability at a given partial oxidation state, the number of coulombs for the re-reduction of the oxidized polymer would be different compared to the initial oxidation.

As stated earlier, the chemical stability at a specific oxidation state was also monitored by DPV. After an oxidation/re-reduction cycle, a DPV was run and compared to that of the uncycled or virgin polymer. The DPV for initially uncycled polymer and the oxidation/re-reduction cycled polymer were essentially identical even after 10 cycles. These results suggest that the polymer is stable at all degrees of oxidation. If the polymer was unstable toward oxidation at a specific potential, the DPV would be expected to show a significant change after the oxidation/re-reduction cycle. This was never observed. The UV/Vis absorption spectra of neutral uncycled virgin polymer (Figure 6) and extensively oxidation/re-reduction cycled neutral polymer, including 100% oxidation (Figure 13), are similar, with no peaks associated with monomeric fragments (Figure 4). Absorbance peaks in the spectra of the neutral uncycled

Figure 13. UV/Vis spectra of the extensively cycled silicon polymer, $(t\text{-}Bu_4PcSiO)_n$, obtained in CH_2Cl_2. Absorbance peaks occur at 625 and 327 nm. The UV/Vis spectra of the extensively cycled silicon polymer is essentially the same as the pristine polymer.

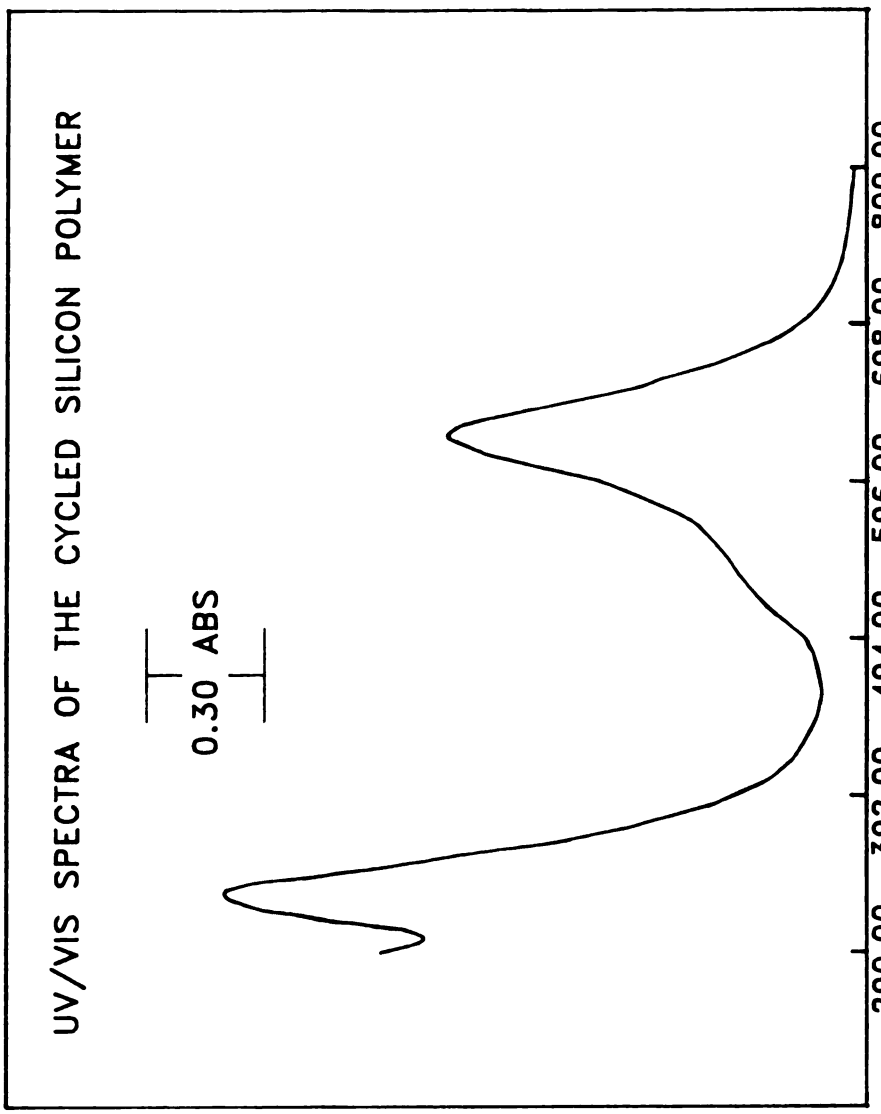
UV/VIS SPECTRA OF THE CYCLED SILICON POLYMER
0.30 ABS
290.00
392.00
494.00
596.00
698.00
800.00
WAVELENGTH (NM)

FIGURE 13

virgin polymer (Figure 6) occurred at 619 and 327 nm. The literature reported wavelengths for the same peaks are 612 and 322 nm.[17a] The extensively cycled polymer has absorbances at 625 and 327 nm, similar to the uncycled polymer and to the literature values. The UV/Vis absorption spectra suggests that the polymer is stable to oxidation/re-reduction cycles.

3.2 Rotating Disk Voltammetry Studies

3.2.1 Introduction

Conventional voltammetric techniques can also be used to characterize the redox properties of the polymer. In rotating disk voltammetry, the working electrode is connected to a motor, which spins the electrode and causes sample to pass by the electrode due to forced convection of the solution. Most voltammetric techniques are performed on quiescent solutions, where diffusion is the main mode of transport of material to and from the electrode. In RDE voltammetry, the rotation of the working electrode causes the rate of mass transfer to be much greater than the rate of diffusion.[24] Thus, during an RDE experiment, electrochemically unperturbed material is continuously being brought up to the electrode due to the rapid transfer of sample by forced convection. The rotation of the working electrode, in conjunction with a slow potential scan rate (10 mv/sec), enables these experiments to be obtained under steady state conditions. The current at any potential is independent of scan direction and time. Although currents in rotating disk voltammetry are typically larger than in other voltammetric techniques (cyclic voltammetry and differential pulse voltammetry), the total current is

small enough that little net electrolysis of the bulk solution occurs. Rotating disk voltammetry was utilized to determine if there were any kinetic limitations to the oxidation of the polymer. The current-potential curve obtained from RDE voltammetry can also be used to obtain the doping profile of the polymer as a function of potential. The RDE experiment provided the same information as an entire series of CPC experiments in a few minutes.

3.2.2 Procedure

Supporting electrolyte ($TBABF_4$) was weighed out and added to the three compartments of the RDE cell. The concentration of supporting electrolyte ($TBABF_4$) in each compartment was enough to produce a 0.2 M solution. A known amount of polymer (11.0-12.0 mg, 0.55-0.60 mg/mL) was weighed out and added to the working compartment. The typical concentration of the polymer in the cell was 2.8×10^{-5} M to 3.2×10^{-5} M based on a 25 phthalocyanine moiety polymer.[17b] The solvent used for these experiments, 1,1,2,2-tetrachloroethane, was vacuum transferred into a solvent transfer tube and then pipetted into the cell in an inert atmosphere glovebag. Prior to electrochemical measurements, the working compartment was extensively deaerated by bubbling with argon. The working electrode, a platinum ring-disk electrode (Pine Instruments, Grove City PA) was polished with 0.05 μm alumina prior to use.

3.2.3 Results

Shown in Figure 14 are a series of rotating disk electrode (RDE) voltammograms of the silicon polymer obtained at different rotation rates. The potential was scanned over the entire range defined by the CPC results. The starting potential was set negative

Figure 14. Rotating disk voltammograms of a 0.0208 mM solution of the silicon polymer, $(t\text{-}Bu_4PcSiO)_n$, in 1,1,2,2-tetrachloroethane / 0.2 M $TBABF_4$ at a Pt disk electrode at different rotation rates. The background RDE voltammogram of a blank solution was obtained at 1800 rpm. The current values for the background RDE did not vary as a function of rotation rate.

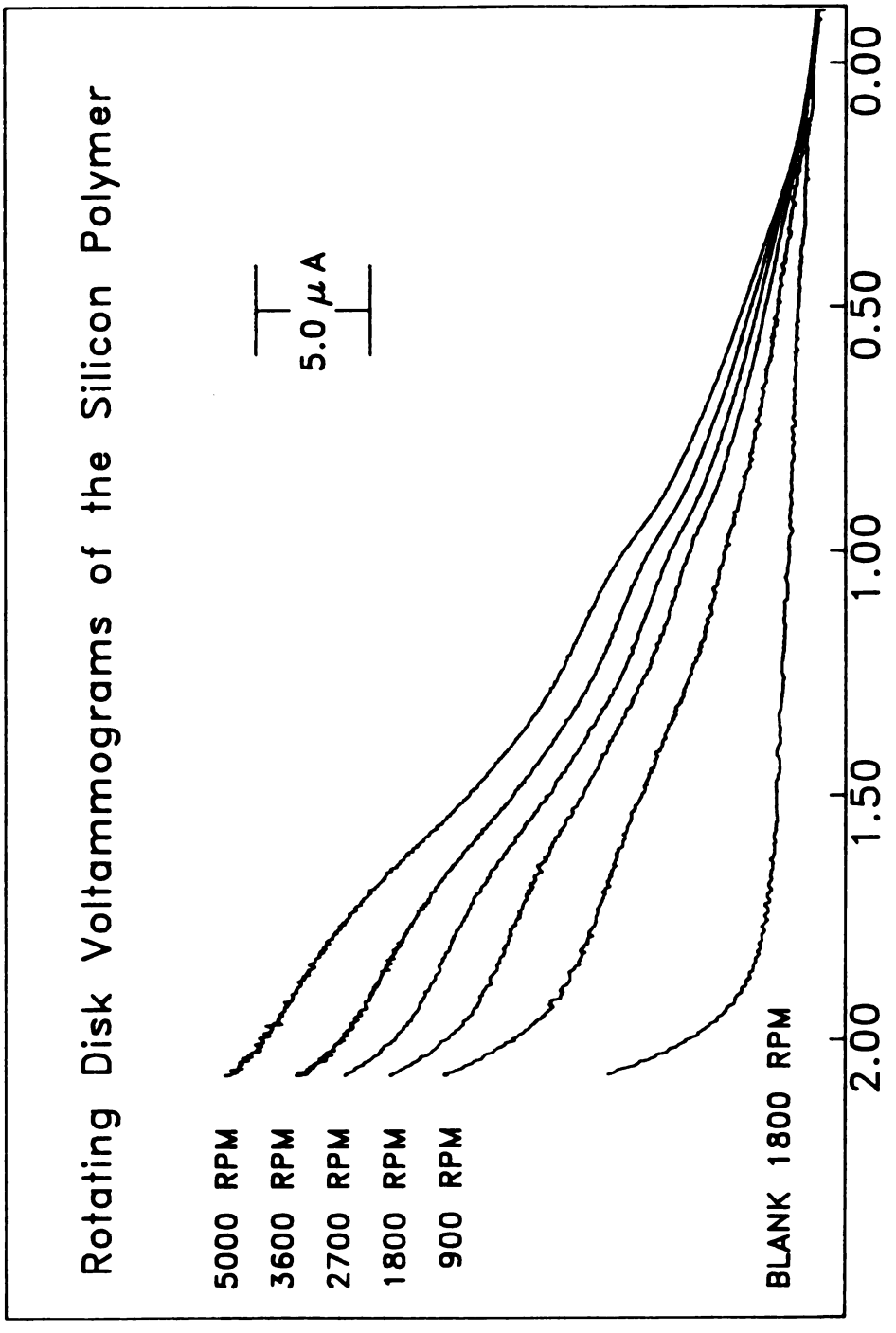
Rotating Disk Voltammograms of the Silicon Polymer
5.0 μA
5000 RPM
3600 RPM
2700 RPM
1800 RPM
900 RPM
BLANK 1800 RPM
2.00
1.50
1.00
0.50
0.00
POTENTIAL (volts vs SSCE)

FIGURE 14

of the initial oxidation response observed in DPV and CPC experiments. The final potential was determined by the oxidation of the solvent. The increase in current at high positive potentials is due to this process. The RDE voltammograms occur over an approximately 1700 mV range, in contrast to a typical rotating disk response for a single conventional redox couple would require approximately 200 mV to change its oxidation state.[24] The general equation which describes the current response for rotating disk voltammetry is:

$$i = \frac{n\,F\,A\,D_o\,[\,C_o^{*} - C_o(y=0)\,]}{1.61\,D_o^{1/3}\,\omega^{-1/2}\,\nu^{1/6}} \qquad (3)$$

where:

ω - angular velocity of the disk ($\omega=2\pi N$, N=rps)

ν - kinematic viscosity of the fluid, $cm^2\ sec^{-1}$

i - current, A

C_o^{*} - initial solution concentration, mol cm^{-3}

$C_o(y=0)$ - solution concentration at the electrode, mol cm^{-3}

D_o - diffusion coefficient, $cm^2\ sec^{-1}$

A - area of the electrode

n - number of electrons

The % oxidation vs. potential plot (Figure 15) for the polymer can also be calculated from the rotating disk voltammograms. The current at 1.82 V (Figure 14) is the limiting current for the rotating disk voltammograms. At this potential, the polymer is assumed to be 100% oxidized (supported by CPC results). The percent oxidation at a given potential, can be calculated from the limiting

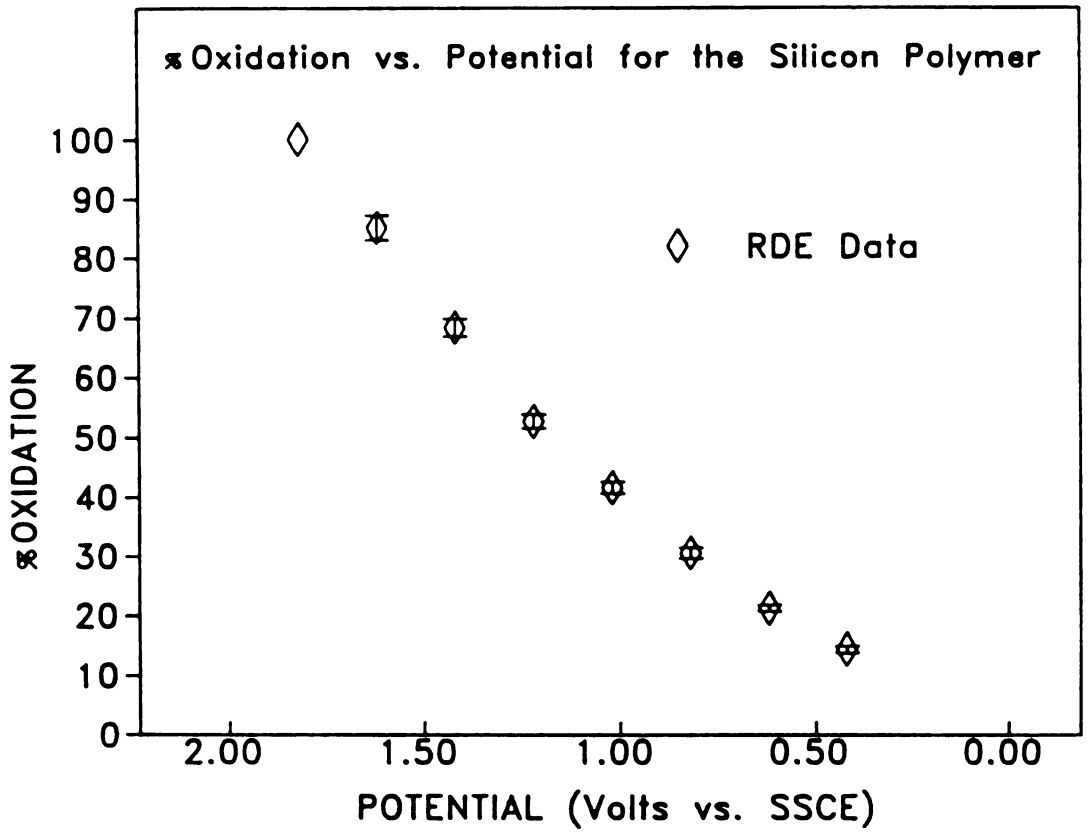

Figure 15. The degree of oxidation vs. potential for the silicon polymer, $(t\text{-}Bu_4PcSiO)_n$, determined from the RDE voltammograms. The RDE values were determined by normalizing the current at any potential to the limiting current at 1.82 V. The error bars represent the standard deviation of the calculated % oxidation, for the same potential, at different rotation rates.

current and the current at that specific potential. The % oxidation is calculated by dividing the current at the given potential by the limiting current and multiplying by 100. Consistent % oxidation vs. potential curves are obtained at all rotation rates. The error bars in Figure 15 represents the standard deviation of the % oxidation vs. potential values calculated from the five individual RDE voltammograms. In addition, as seen in Figure 15 (% oxidation vs. potential for RDE and CPC), there is excellent agreement between the two inherently different techniques for the determination of the % oxidation vs. potential curve. The shape of the RDE voltammograms are independent of angular frequency ($\omega=2\pi N$, N = rps) and increase in magnitude with $\omega^{1/2}$. This behavior is predicted only for a reversible, nernstian redox system. The magnitude of the limiting current is described by the Levich equation.

3.2.4 Levich Plot

If there is no kinetic barrier to electron transfer, the increase in current for rotating disk voltammetry is dependent only on the increase in rotation rate ($\omega^{1/2}$).[24a] The equation that

describes the limiting current for a rotating disk voltammogram is given by the Levich equation.

$$i_L = 0.620\ n\ F\ A\ C_o\ D_o^{2/3}\ \nu^{-1/6}\ \omega^{1/2} \qquad (4)$$

where:

ω - angular velocity of the disk (ω=2πN, N=rps)

ν - kinematic viscosity of the fluid, $cm^2\ sec^{-1}$

i_L - limiting current, A

C_o - solution concentration, mol cm^{-3}

D_o - diffusion coefficient, $cm^2\ sec^{-1}$

A - area of the electrode

n - number of electrons

For a specific redox system, all of the terms in the Levich equation are constant except i_L and $\omega^{1/2}$. The current, at any potential, should vary as $\omega^{1/2}$. A plot of i(E) vs. $\omega^{1/2}$ for a reversible system should yield a straight lines that intersect the origin. A deviation from a straight line suggests a kinetic limitation or barrier for the electron transfer reaction. A plot of current vs. $\omega^{1/2}$ (Figure 16), does in fact yield straight lines that intersect the origin at all potentials for the doping process. The deviation at the high potential values is probably due to the oxidation of the solvent. The straight line behavior is indicative of a simple, uncomplicated charge transfer process, and suggests that there are no kinetic

Figure 16. Plot of disk current at various potentials and rotation rates vs. $\omega^{1/2}$ ($\omega = 2\pi N$, N=rps), for the oxidation of the silicon polymer, $(t\text{-}Bu_4PcSiO)_n$, in 1,1,2,2-tetrachloroethane/0.2 M $TBABF_4$.

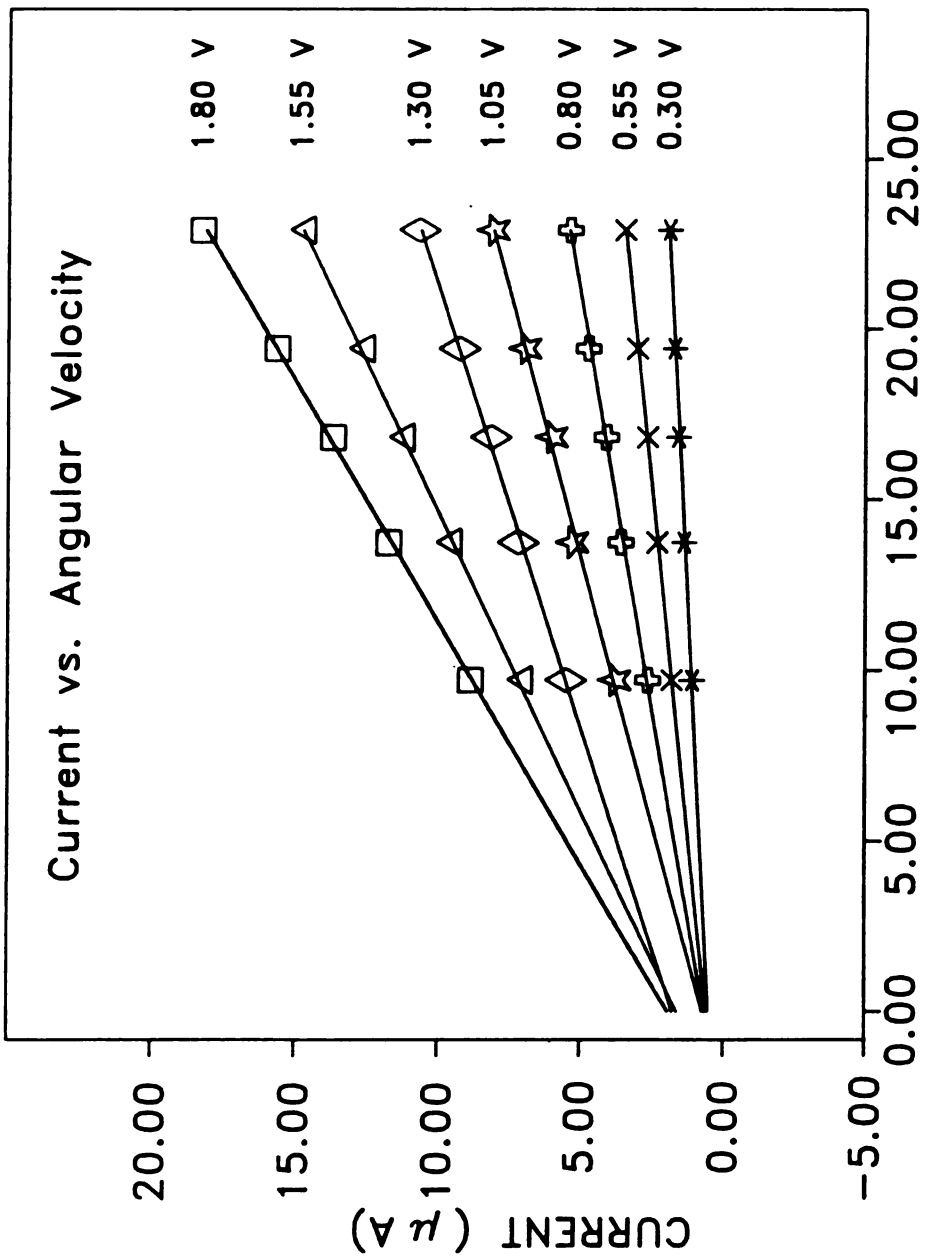
Current vs. Angular Velocity
1.80 V
1.55 V
1.30 V
1.05 V
0.80 V
0.55 V
0.30 V
CURRENT (μA)
20.00
15.00
10.00
5.00
0.00
-5.00
0.00
5.00
10.00
15.00
20.00
25.00
SQR of ANGULAR FREQ.

FIGURE 16

limitations for the oxidation of the polymer. Thus, charge can be easily removed from the polymer at all levels of oxidation.

3.3 Differential Pulse Voltammetry

3.3.1 Introduction

Differential pulse voltammetry (DPV), a very sensitive derivative technique was also used to characterize the redox response of the silicon polymer. DPV is an attractive technique for studying multi-electron transfer events due to its high sensitivity and resolution. Unlike the featureless response observed for most voltammetric techniques, DPV is extremely sensitive to subtle changes in the doping profile. DPV was employed in hopes of observing the individual redox states comprising the polymer.

3.3.2 Procedure

The differential pulse voltammetry experiments were performed in a single compartment cell. The working electrode was a small area Pt electrode (BAS Inc., W. Lafayette, IN) that was polished prior to use with 0.05 μm alumina. Enough supporting electrolyte ($TBABF_4$) was weighed out and placed in the cell to provide a 0.2 M solution. A known amount of polymer was weighed out and placed in the cell to provide a 0.55-0.60 mg polymer/mL solution. The polymer was placed in a dumpster, a rotatable reservoir that allowed the addition of polymer at any time. Utilizing this dumpster, voltammograms of the blank solution could also be obtained. These background voltammograms could then be subtracted from sample voltammograms to obtain

background corrected data. The background voltammograms were also useful in determining the potential window of the solvent.

3.3.3 Results

Shown in Figure 17 is a DPV of the $(t\text{-}Bu_4PcSiO)_n$ polymer. The DPV response of the polymer is approximately 1700 mV wide, which is similar to that obtained by CPC and RDE experiments. In contrast, a DPV of a single non-interacting redox couple, for example ferrocene, would typically have a base peak width about 200 mV wide.[24a,26] The 1700 mV potential width of the polymer's differential pulse voltammogram is indicative of a material with multiple interacting redox sites. These multiple interacting redox sites provide a large energy range of states from which charge can be removed. The DPV observed for the polymer does not have a symmetrical response. The DPV shows an onset of current at 0.15 V, rising to a peak around 0.7 V, where it then dips sharply. The current levels off at 1.00 V and then begins to increase sharply to a current maximum at 1.55 V. After this current maximum, the current decays to background levels, suggesting that no further oxidation is occurring. The current dip at 1.00 V occurs after approximately 45% oxidation based on controlled potential coulometry data. This nonlinear doping profile is indicative perhaps of some stability or reorganization for the polymer occurring at or near 45% oxidation.[27] The steady increase in current from 1.00 V to the maximum at 1.55 V is indicative of a greater density of states in that potential region than in the region from 0.15 V to 0.95 V. While DPV is one of the most sensitive electrochemical techniques, it did not provide any information on the individual redox potentials of states in the polymer. The degree of

Figure 17. Differential pulse voltammogram of a 0.056 mM solution of silicon polymer, $(t\text{-}Bu_4PcSiO)_n$, in 1,1,2,2-tetrachloroethane / 0.2 M $TBABF_4$ obtained with a small area 0.018 cm^2 Pt electrode. The scan rate was 4 mV/s, pulse amplitude = 50 mV, pulse width = 50 ms, and the pulse period = 1000 ms.

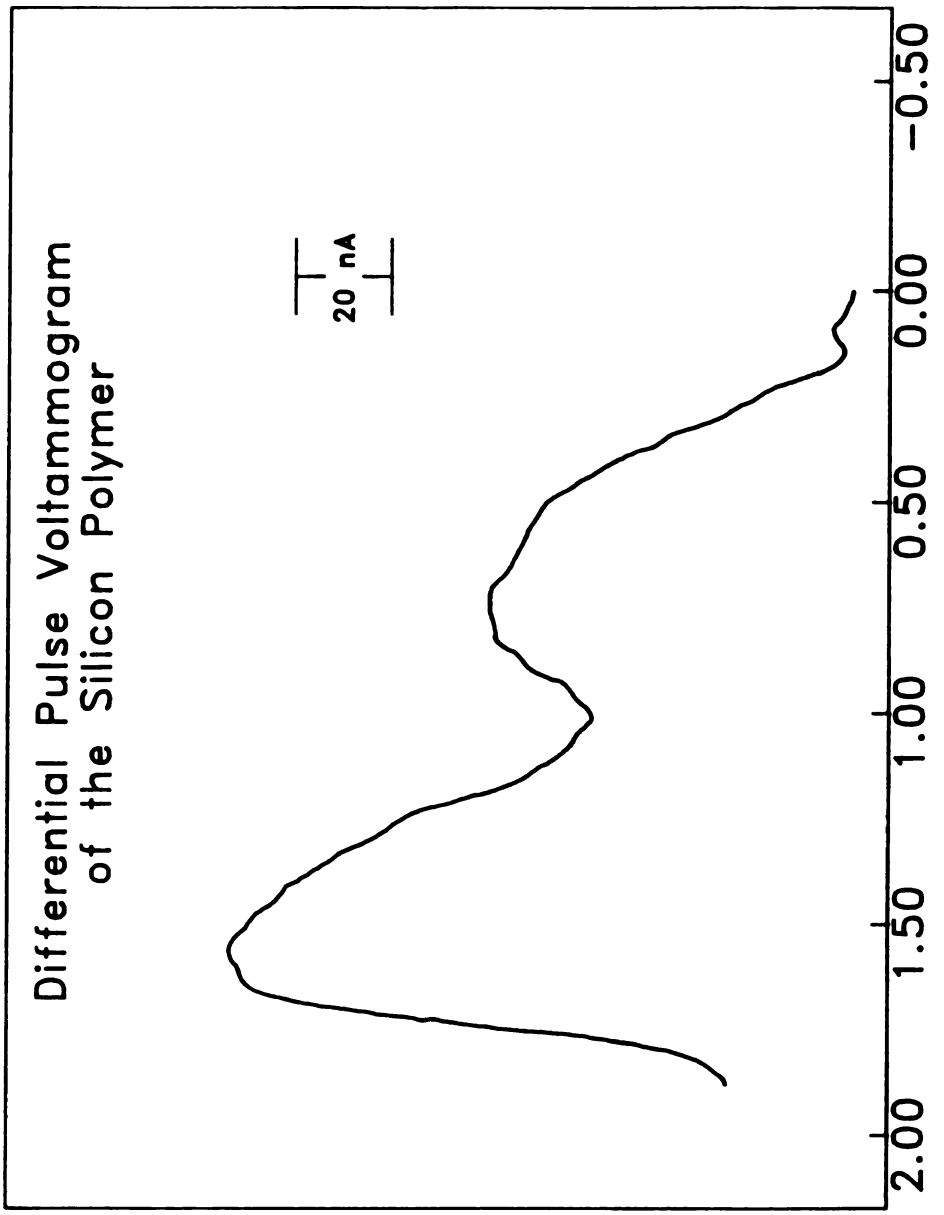
Differential Pulse Voltammogram
of the Silicon Polymer
20 nA
2.00
1.50
1.00
0.50
0.00
-0.50
POTENTIAL (volts vs SSCE)

FIGURE 17

polymerization of the silicon polymer (n = 25) has been determined from end group analysis and is reported in the literature.[17b] This information, along with the concentration of the polymer, area of the electrode, diffusion coefficient of the polymer, and the potential pulse sequence employed, determine the potential-current response. These experimental parameters were used as variables in a digital simulation, so that the experimental current-potential DPV response of the polymer could be modeled.

3.3.4 Digital DPV Simulation

The model utilized for the digital simulation of the DPV response of the polymer, is based on sequential electron transfer of redox couples in equilibrium with one another (see Appendix A). This is exactly analogous to the sequential proton transfer in polyprotic acids.[28] The ultimate goal of the digital simulation was to estimate the approximate redox potentials of sites in the polymer, their distribution, and to obtain some information on the current dip at 1.00 V (corresponding to 45% oxidation). The modeling of the DPV current potential response should also provide information on the chainlength of the polymer. The computer program is based on the finite differences method and initially divides the solution up into a number of volume elements or boxes.[29] The program simulates diffusion between the volume elements and calculates the surface and bulk conditions of each redox state of the polymer. The initial and bulk concentrations are the same as the experimental values in Figure 17. The next step is to set up the conditions at the working electrode and to calculate the dimensionless current. The program then goes back and recalculates the diffusion of material to and from

the electrode. The program executes these steps continuously until the final potential of the experiment is reached. The ratio of reactant and product concentrations at the electrode surface is based the Nernst equation and is a function of electrode potential. The number of states in the polymer that are oxidized is dependent solely on the standard potentials of the sites and the potential of the working electrode. The current is calculated from the flux of the polymer at the electrode surface and number of states of the polymer being oxidized. The potential of each individual redox state in the polymer was inputted into the computer program (Table 2) along with the other experiment parameters necessary for the simulation. The digital simulation utilized the same experimental conditions and parameters as those used to acquire the DPV shown in Figure 17. The digital DPV simulation, Figure 18, is very similar to the experimental DPV of the silicon polymer, Figure 17. The simulation program was run numerous times on a trial and error basis to achieve the best fit between the real and simulated data. After the simulation was run several times, the response of various changes in the parameters could be predicted. A more rational, calculating approach was then taken to the refining of the simulated DPV. The shape of the simulated DPV is extremely sensitive to the standard potentials chosen for the redox couples used to model the polymer. Small changes in the distribution of these values caused drastic changes in the current-potential shape of the simulated DPV. From the simulation, information is obtained about the standard potential of the sites in the polymer. The experimental and simulation DPV, Figures 17 & 18, are very similar in their current-potential shapes.

TABLE II

Digital Simulation Data for the Silicon Polymer

Redox Site	Standard Potential (E^0)[a]	Potential Difference Between Successive Sites[b]
1	0.275	
		9.0
2	0.365	
		8.5
3	0.450	
		8.0
4	0.530	
		7.5
5	0.605	
		7.0
6	0.675	
		6.9
7	0.744	
		6.7
8	0.811	
		6.4
9	0.875	
		7.0
10	0.945	
		7.5
11	1.020	
		11.0
12	1.130	
		8.0
13	1.210	
		6.6
14	1.276	
		5.4
15	1.330	
		5.0
16	1.380	
		4.7
17	1.427	
		4.4
18	1.471	
		4.2
19	1.513	
		4.1
20	1.554	
		4.0
21	1.594	
		4.0
22	1.634	
		4.1
23	1.675	
		4.4
24	1.719	
		5.5
25	1.774	

[a] in volts (V).

[b] in millivolts (mV).

Figure 18. Simulated differential pulse voltammogram for the oxidation of the silicon polymer. The conditions utilized (scan rate, pulse width, concentration, pulse amplitude, area of electrode) for the simulation are the same as those of the experimental data shown in Figure 13. The bars along the X-axis represent the standard potentials of the redox couples utilized to obtain the current-potential response (see Table 2 for the exact potentials).

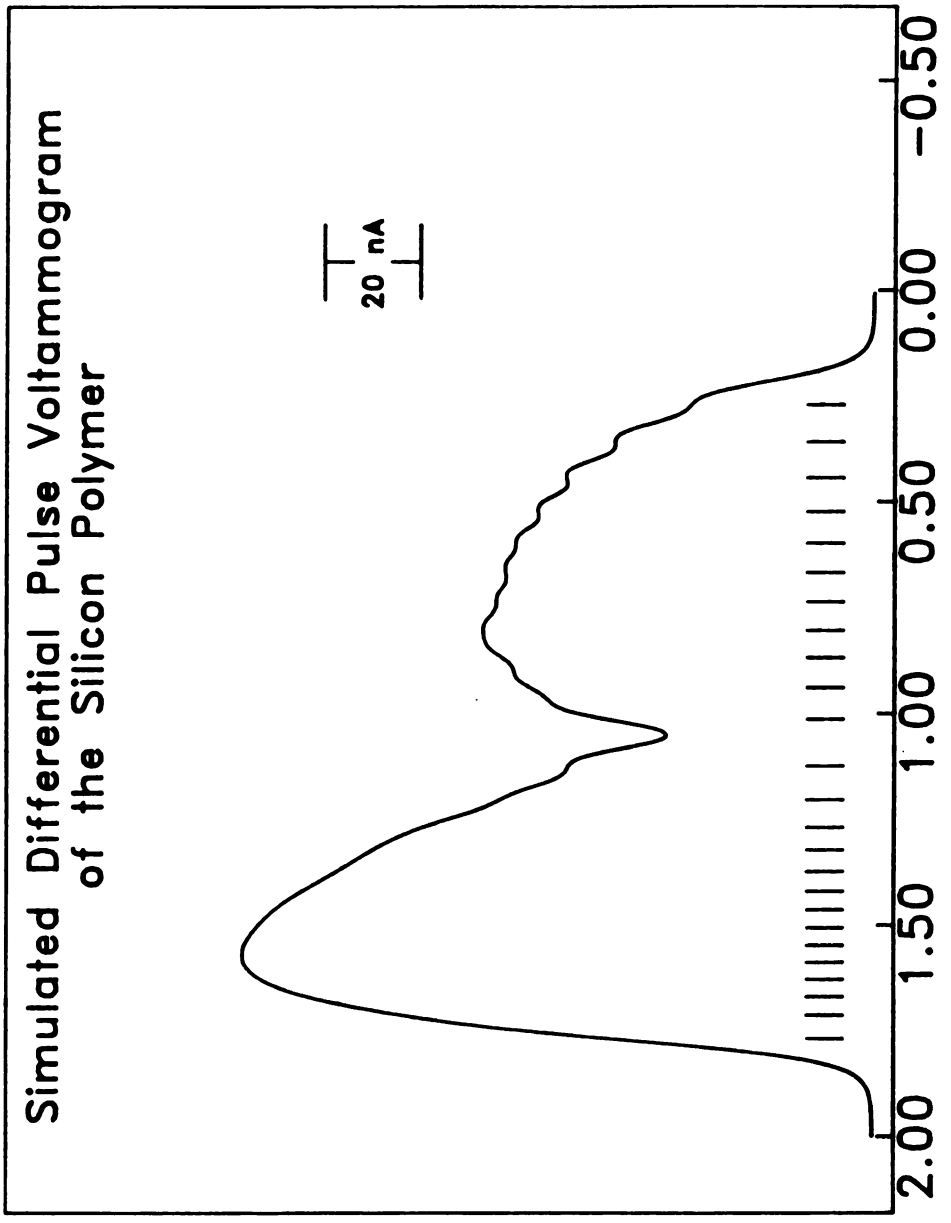
Simulated Differential Pulse Voltammogram
of the Silicon Polymer
20 nA
2.00
1.50
1.00
0.50
0.00
-0.50
POTENTIAL (volts vs SSCE)

FIGURE 18

Thus, the redox potentials used in the digital simulation approximately match the states in the polymer. Information obtained from the distribution of the redox states in the simulation is quite interesting. Shown in Figure 19 is a plot of the difference in potential between successive sites used in the DPV simulation. The difference in potential initially between the sites is approximately 9 mV. The potential difference between successive sites then steadily decreases to 6.4 mV between sites 8 and 9. The difference in potential then increases with a substantial gap of 11 mV between site 11 and 12, this corresponds to a current gap in the simulation similar to the experimental DPV dip at 1.00 V. After the dip a 1.00 V, the potential difference between successive sites slowly decreases in a smooth transition. The smallest potential difference is found between sites 20, 21, and 22 which are only 4 mV apart. The potential difference for the remaining sites increase slightly to a final potential difference of 5.5 mV between sites 24 and 25. The % oxidation vs. potential for the polymer (Figure 20) was also calculated based on this sequential electron transfer model. These values are determined assuming a nernstian distribution of species dependent on the electrode potential. The concentration of the unperturbed and oxidized states in the polymer was calculated from the Nernst equation knowing the redox potential of each site and the potential of the working electrode. Shown in Figure 21 is a plot of % oxidation vs. potential from CPC experiments and the digital DPV

Figure 19. A plot of the difference in standard potential between successive sites utilized in the DPV, CV, and RDE simulations of the silicon polymer (see Table 2 for the exact values).

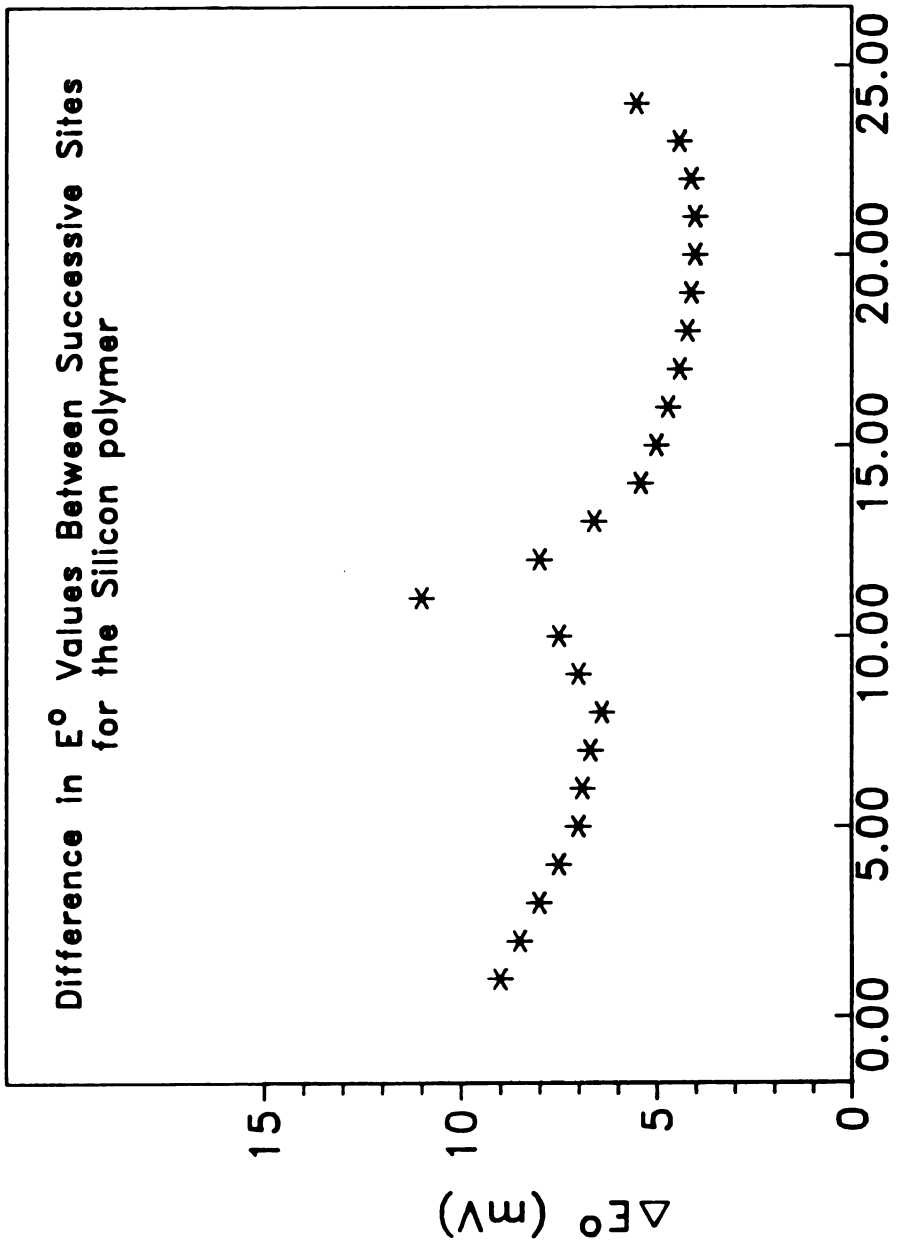
Difference in E° Values Between Successive Sites
for the Silicon polymer
ΔE° (mV)
SITE NUMBER
0
5
10
15
0.00
5.00
10.00
15.00
20.00
25.00

FIGURE 19

Figure 20. The degree of oxidation vs. potential calculated by digital simulation using the potentials listed in Table 2. The % oxidation is not calculated from a particular technique, rather it is based on the number of sites oxidized at a specific potential. The number of sites oxidized is determined from the potential of the electrode, the standard potential of the sites, and the Nernst equation (see also Appendix A).

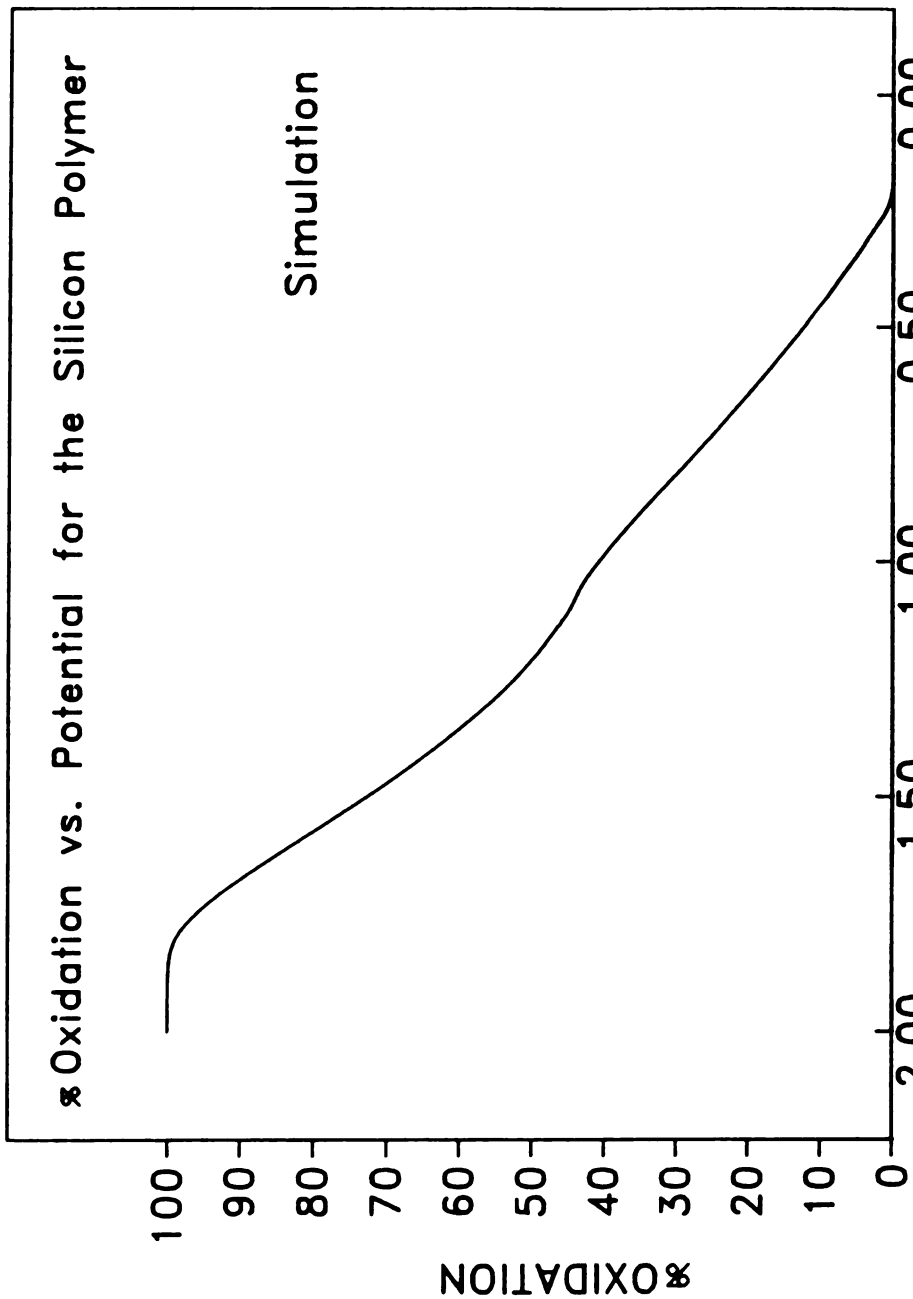
% Oxidation vs. Potential for the Silicon Polymer
Simulation
% OXIDATION
100
90
80
70
60
50
40
30
20
10
0
2.00
1.50
1.00
0.50
0.00
POTENTIAL (Volts vs. SSCE)

FIGURE 20

Figure 21. The degree of oxidation vs. potential for the silicon polymer, $(t\text{-}Bu_4PcSiO)_n$, from the CPC data and the digital simulation.

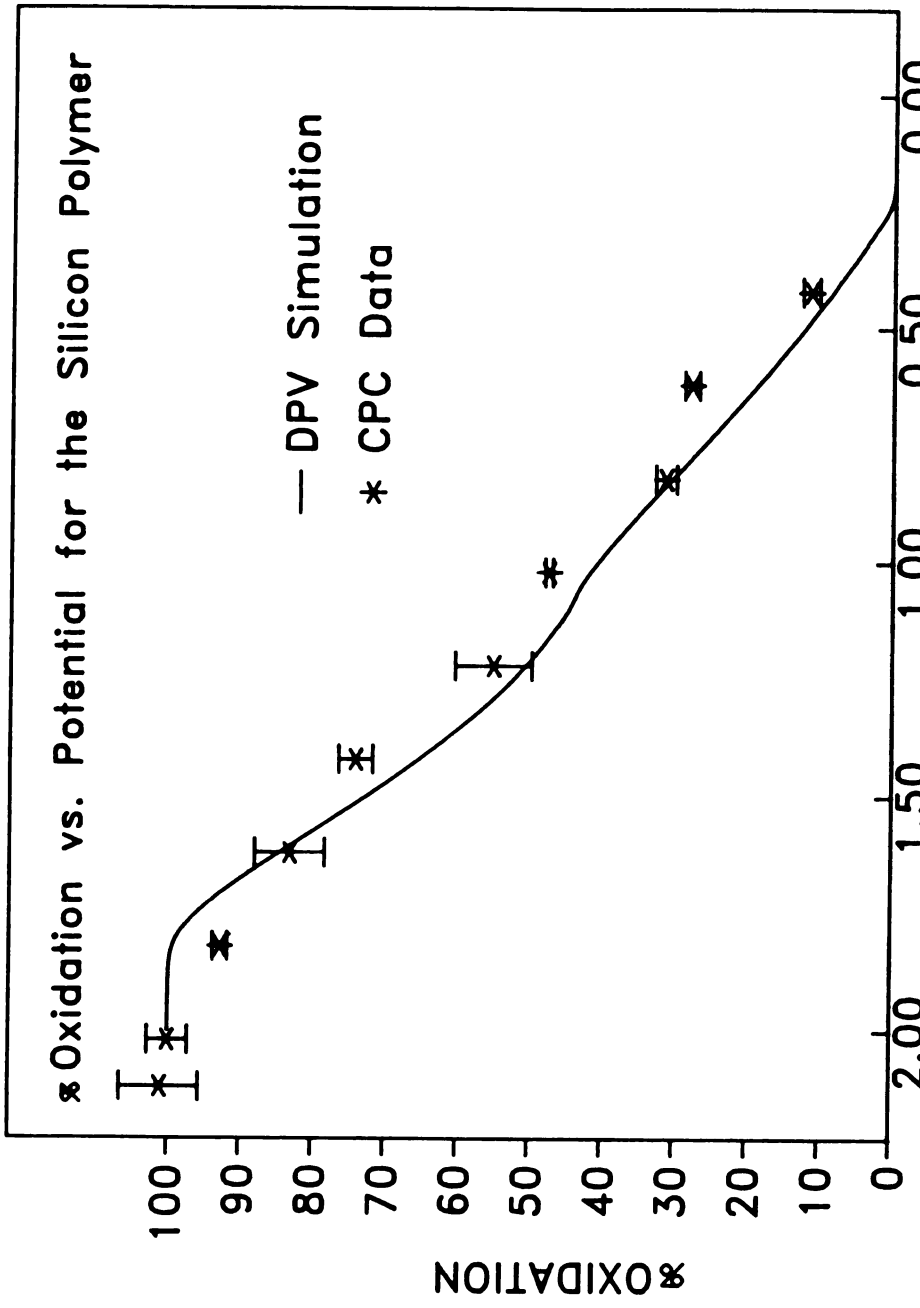
% Oxidation vs. Potential for the Silicon Polymer
— DPV Simulation
* CPC Data
%OXIDATION
100
90
80
70
60
50
40
30
20
10
0
2.00
1.50
1.00
0.50
0.00
POTENTIAL (Volts vs. SSCE)

FIGURE 21

simulation. There is excellent agreement between the two sets of data.

3.4 Cyclic Voltammetry

3.4.1 Introduction

Cyclic voltammetry (CV) has also been utilized in the study of the silicon polymer. In this particular technique, the potential is cycled from some initial potential to a switching potential and then back to the initial potential at a constant sweep rate. From the cyclic voltammogram or current-potential response, several different characteristics of the system being probed can be determined. From the peak splitting of the anodic and cathodic peaks, the number of electrons involved in the redox event can be determined.[24] The stability of reactants and/or products, and kinetic information regarding the electron-transfer reaction can be probed by varying the sweep rate. Products of a redox event that decompose can be "captured" and potentials required for their oxidation or reduction can be determined. These traits have made cyclic voltammetry one of the most widely used electrochemical techniques.

3.4.2 Procedure

Cyclic voltammetry studies were carried out in a one compartment cell, identical to that used for DPV studies. The procedure for the experiment is the same as for DPV (see section 3.3.2).

3.4.3 Results

Shown in Figure 22, is a typical cyclic voltammogram (CV) of the silicon polymer. The current is relatively high, however, there

Figure 22. Cyclic voltammogram of a 0.0432 mM solution of silicon polymer, $(t\text{-}Bu_4PcSiO)_n$, in 1,1,2,2-tetrachloroethane / 0.2 M $TBABF_4$ obtained with a small area 0.018 cm^2 Pt electrode. The scan rate was 100 mV/s.

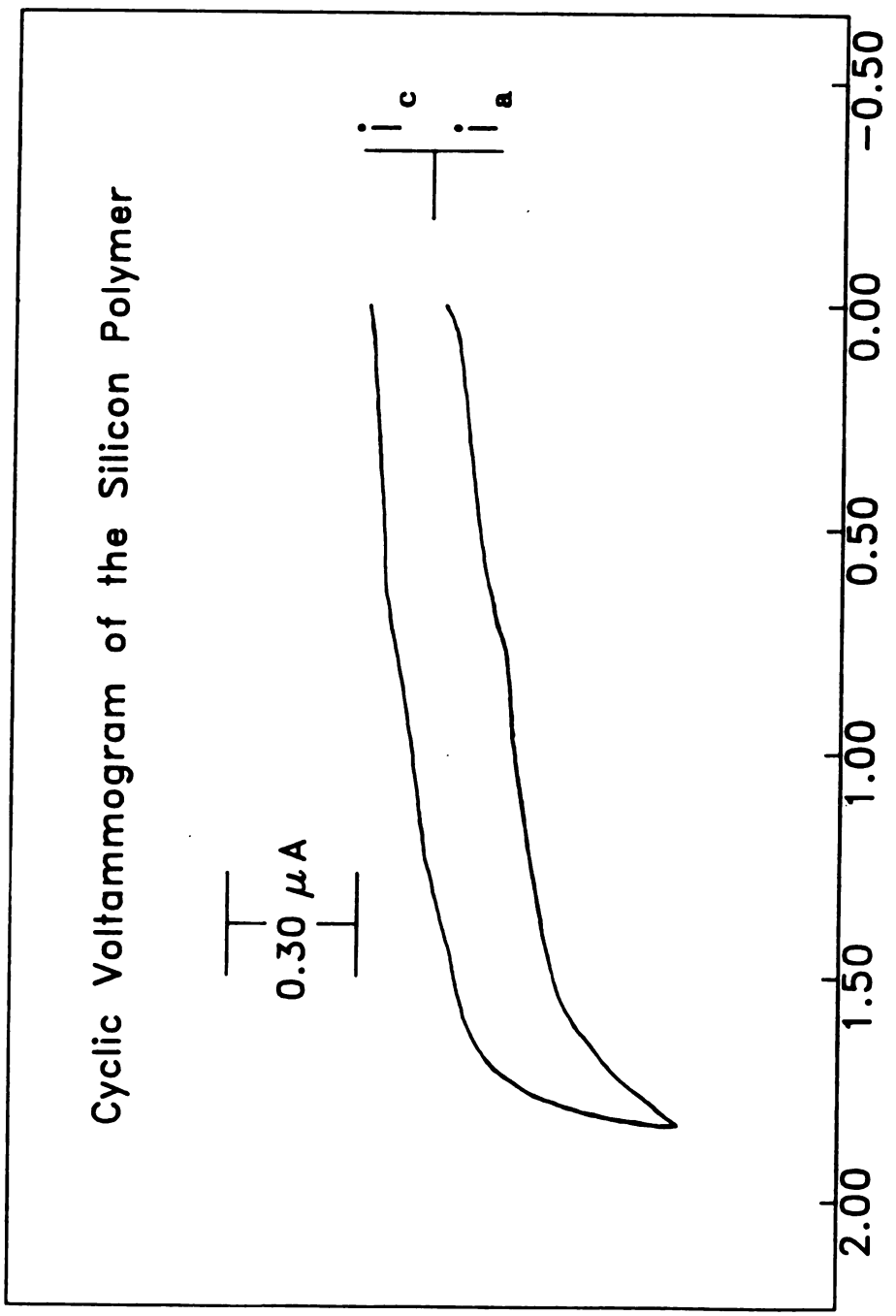
Cyclic Voltammogram of the Silicon Polymer
0.30 μA
i_c
i_a
2.00
1.50
1.00
0.50
0.00
−0.50
POTENTIAL (volts vs SSCE)

FIGURE 22

are almost no discernable features. The CV is extremely smooth and broad, very similar to a background voltammogram. In contrast, observe the CV of the bis(trimethylsilyloxy)(tetra-t-butylphthalocyaninato)silicon, the capped-monomer [(t-Bu_4PcSiO_2)($Si(CH_3)_3)_2$], Figure 23. The CV of the capped monomer shows two reversible oxidation waves. The CV of the monomer shows the typical current-potential shape, a large anodic current (oxidation) and after potential reversal, a large cathodic current (reduction). The peak splitting of the wave should only be approximately 60 mV/n apart for a reversible system, and in fact the peak splitting is close to this value.[24a] The capped monomer actually undergoes two one electron oxidations separated by 900 mV, forming the stable monocation and dication as shown by the reversibility of the CV. The CV of the polymer can be digitally simulated using a program very similar to that used for the digitally simulated DPV (see section 3.3.4). Both electrochemical simulation programs are structured the same way, utilizing the finite differences method and modeled based on sequential electron transfer between states in equilibrium with one another. In Figure 24, the digitally simulated current-potential curve of the polymer, shows a CV which is very similar to the experimentally observed voltammogram. The potentials used for the simulation are the same values used for the DPV simulation (Table 2). The CV shows very little information

Figure 23. Cyclic voltammogram of a 1.25 mM solution of bis(trimethylsiloxy)(tetra-t-butylphthalocyaninato)silicon, (t-Bu_4PcSiO_2)($Si(CH_3)_3$)$_2$, the capped monomer in 1,1,2,2-tetrachloroethane / 0.2 M $TBABF_4$ obtained with a 0.018 cm^2 Pt electrode. The scan rate was 100 mV/s.

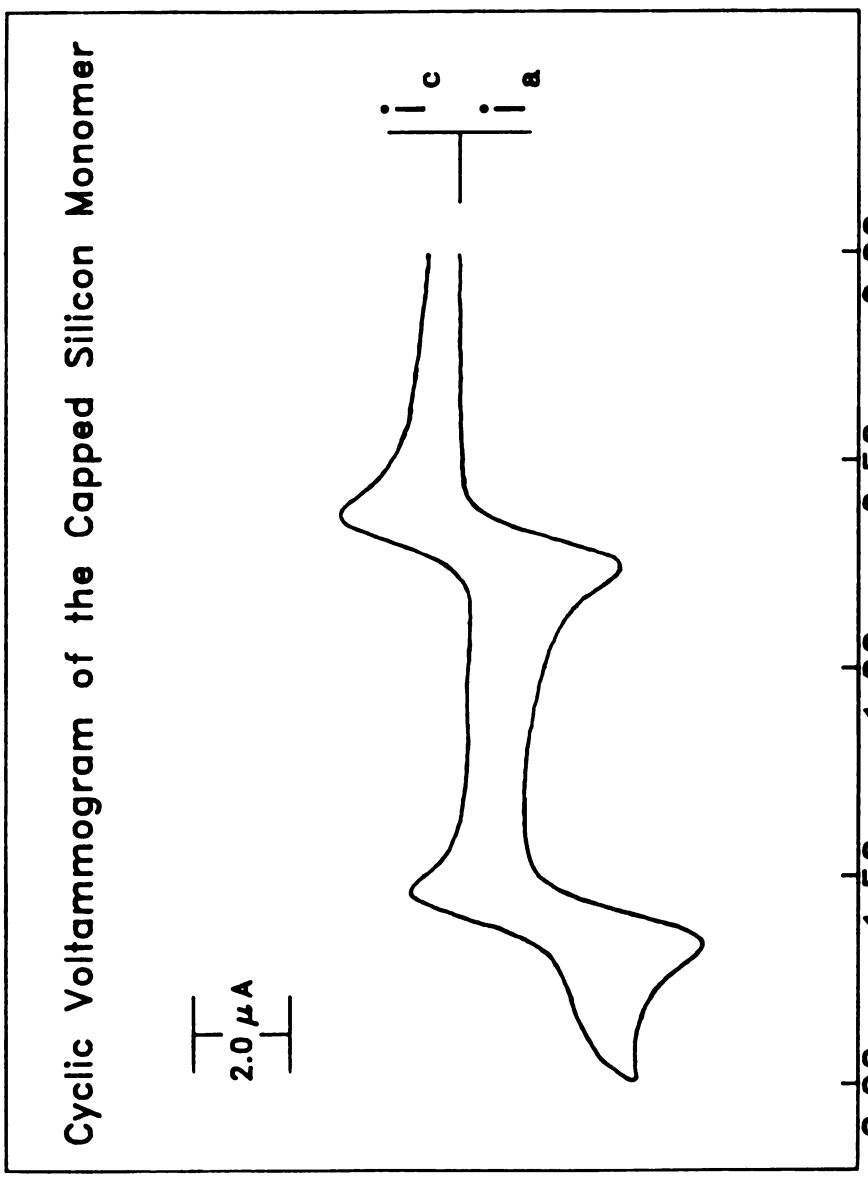
Cyclic Voltammogram of the Capped Silicon Monomer
2.0 μA
i_c
i_a
2.00
1.50
1.00
0.50
0.00
POTENTIAL (volts vs SSCE)

FIGURE 23

Figure 24. Simulated cyclic voltammogram of the oxidation of the silicon polymer. The standard potentials used in this simulation are the same as those used for Figure 13 (see Table 2 for the exact potentials). The conditions utilized (scan rate, concentration, area of electrode) are the same as those in Figure 18.

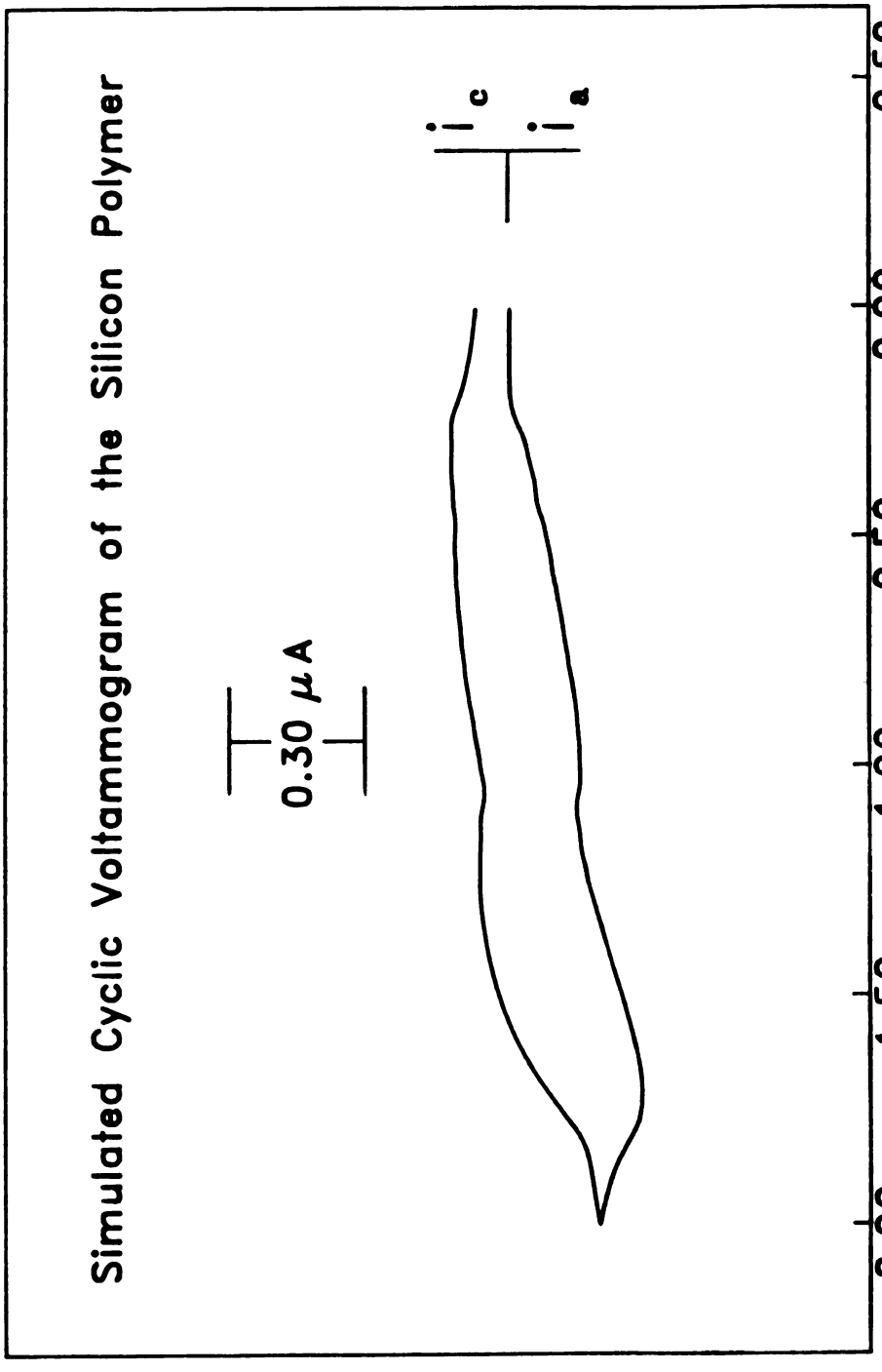
Simulated Cyclic Voltammogram of the Silicon Polymer
0.30 μA
i_c
i_a
2.00
1.50
1.00
0.50
0.00
-0.50
POTENTIAL (volts vs SSCE)

FIGURE 24

due to the close proximity of the redox states in the polymer. The broad featureless CV is actually the response expected.

3.5 Chronocoulometry

3.5.1 Introduction

Chronocoulometry is an electrochemical technique where the potential of the working electrode is stepped from an initial potential where no faradaic current flows to a final value where electron transfer occurs.[24a] In most cases the potential of the electrode is set well past the half wave potential of the redox couple to give a diffusion-limited current. The potential of the electrode is kept constant for a specific length of time, and the resultant charge is measured.

3.5.2 Procedure

Chronocoulometry studies were carried out in a one compartment cell, identical to that used for DPV studies. The procedure for the experiment is the same as for DPV (section 3.3.2).

3.5.3 Results

The diffusion coefficient of the polymer was determined from chronocoulometry experiments. The integrated Cottrell equation, which describes the amount of charge passed as a function of time, was used to determine the diffusion coefficient of the polymer. The potentials utilized for the experiment were obtained after consulting the DPV response of the polymer. The initial starting potential of the experiment, was a potential where no redox response was observed in the DPV of the silicon polymer. The final potential, was a value where the DPV response indicated that no further oxidation of the

polymer was occurring. In the equation below, all of the parameters were known, except for the diffusion coefficient of the polymer. Typical values for a chronocoulometry experiment of the silicon polymer are shown below.

$$Q_d = 2\ n\ F\ A\ C_o\ D_o^{1/2}\ t^{1/2\ \ -1/2} \qquad (5)$$

where:

C_o	= concentration of the polymer, mol cm^{-3}	(6.08×10^{-8})
D_o	= diffusion coefficient, $cm^2\ sec^{-1}$	(?)
A	= area of the electrode, cm^2	(.018)
n	= number of electrons	(25)
F	= Faraday's constant, C mol^{-1}	(96485)
t	= time of the experiment, s	(2)
Q_d	= charge, C	(2.1×10^{-6})

A diffusion coefficient of 2.47×10^{-7} $cm^2\ sec^{-1}$ was calculated from the experimental data. The net charge was obtained by subtracting the charge obtained from a blank solution, from the charge obtained from the polymer solution.

The diffusion coefficient of bis(trimetylsilyloxy)(tetra-t-butylphthalocyaninato)silicon, the capped monomer [(t-Bu_4PcSiO_2)($Si(CH_3)_3)_2$], was also determined by the chronocoulometry technique. The potential utilized for the experiment was obtained after consulting the CV response of the capped monomer. The initial starting potential of the experiment, was a potential where no redox response was observed in the CV. The final potential of the chronocoulometry experiment was at a potential positive of the

potential required for the first one electron oxidation. The same equation used to calculate the diffusion coefficient of the polymer is used for the capped monomer. Typical values for a chronocoulometry experiment of the capped monomer are listed below.

$$Q_d = 2\ n\ F\ A\ C_o\ D_o^{1/2}\ t^{1/2}\ ^{-1/2} \qquad (6)$$

where:

C_o	= concentration of $[(t\text{-}Bu_4PcSiO_2)(Si(CH_3)_3)_2]$, mol cm^{-3}	(1.25×10^{-6})
D_o	= diffusion coefficient, $cm^2\ sec^{-1}$	(?)
A	= area of the electrode, cm^2	(.018)
n	= number of electrons	(1)
F	= Faraday's constant, C mol^{-1}	(96485)
t	= time of the experiment, s	(2)
Q_d	= charge, C	(5.97×10^{-6})

A diffusion coefficient of 2.97 X 10^{-6} cm^2 sec^{-1} was calculated from the experimental data. This calculated diffusion coefficient is very similar to diffusion coefficients of unsubstituted phthalocyanines reported in the literature.[19c]

The relationship between molecular weight and diffusion coefficient for a monomer and the corresponding polymer has been established from both an experimental and a theoretical viewpoint[26c,28]. The diffusion coefficients of the capped monomer and polymer, along with the molecular weights of the capped monomer and repeat unit of the polymer can be used to determine the degree of polymerization. From previous electrochemical studies of the small

length silicon phthalocyanines oligomers (monomer thru tetramer), it is known that significant interaction occurs between the phthalocyanine rings.[17] This suggests that the cofacial arrangement is maintained in solution. Therefore, assuming that the silicon polymer also maintains a cofacial, rod-like structure in solution, the equation that relates diffusion coefficients to molecular weights for the monomer and polymer is:[29b]

$$D_p/D_m = (M_m/M_p)^{0.81} \quad (7)$$

where:

D_p = diffusion coefficient of the polymer 2.47 x 10^{-7} cm^2 s^{-1}

D_m = diffusion coefficient of the monomer 2.97 x 10^{-6} cm^2 s^{-1}

M_m = molecular weight of the monomer = 943.4 g mol^{-1}

M_p = molecular weight of the polymer = ?

The formula of the monomer is $C_{54}H_{66}N_8Si_3O_2$ resulting in a molecular weight of 943.4 g mol^{-1}. The repeat unit of the silicon polymer, $C_{48}H_{48}N_8SiO$, gives a molecular weight of 781.1 g mol^{-1}. Solving the above equation for the molecular weight of the polymer, one obtains a value of 2.038 x 10^4 grams $mole^{-1}$. By dividing the molecular weight of the polymer by the molecular weight of the repeat unit, the degree of polymerization can be calculated. The degree of polymerization obtained is 26.1, this shows excellent agreement with the value reported in the literature and the one used in the digital simulations.[17b].

4. Conclusions

Electrochemical methods can be utilized in the study of soluble electrically conductive materials. The electrochemical response of a soluble electrically conductive material is very different from that of a common non-interacting redox couple. The interaction between adjacent molecules causes widespread changes in the electrochemical response of the electrically conductive material. The oxidation of the silicon polymer occurs over a 1700 millivolt range as seen in the RDE, CPC, and DPV results. A non-kinetically limited conventional redox couple or polymer comprised of non-interacting centers typically has a several hundred millivolt response.[26c] The typical response of a conventional redox couple, for example the capped monomer, is not the same as observed for a conductive material. Conductive materials have a wide range of energetically closely spaced redox states from which charge can either be added or removed.

The partial oxidation for the soluble silicon polymer can be accurately and systematically varied to obtain any value from 0 to 100%, by simply changing the potential of the working electrode. The $(t\text{-}Bu_4PcSiO)_n$ polymer is chemically stable at all degrees of partial oxidation, occurs over a 1700 mV range, and undergoes a simple charge transfer reaction at the electrode. The smooth doping profile along with this broad oxidation process, is indicative of a material with interactive redox sites. The polymer is also stable to repetitive oxidation/re-reduction cycles. The polymer can be cycled to the 100% level and back to the 0% level (neutral polymer), the polymer can

then be oxidized to any previous percent oxidation with no loss or gain in polymer redox activity. Repeat measurements at the same potential provide the same percent oxidation vs. potential values obtained initially. The solubility of the silicon polymer in common non-aqueous solvents, permits the doping process to be unaffected by structural changes which occur in the insoluble unsubstituted species.[15] The small difference in charge between the oxidation and subsequent re-reduction for the CPC results suggests, that there is no inherent stability at any particular oxidation state. The RDE, CPC, and digital simulation (based on an experimentally obtained DPV) experiments all provide remarkably similar results. As seen in Figure 25, the three fundamentally different techniques provide essentially the same percent oxidation vs. potential curve. The excellent agreement between these three techniques, suggests that the potentials for specific levels of partial oxidation are accurately known. These experiments have effectively mapped out the thermodynamic potentials for the oxidation of the polymer.

From an analysis of the rotating disk voltammograms, the oxidation of the silicon polymer was determined to be limited by the mass transport of the material to the electrode and not to a kinetic limitation. This was determined from a Levich plot, where the current was plotted as a function of the square root of angular velocity. The RDE voltammograms also provide information similar to that obtained by CPC results. The CPC results took approximately 24

Figure 25. Degree of oxidation vs. potential for the silicon polymer, $(t\text{-}Bu_4PcSiO)_n$, from the CPC, RDE, digital simulation results.

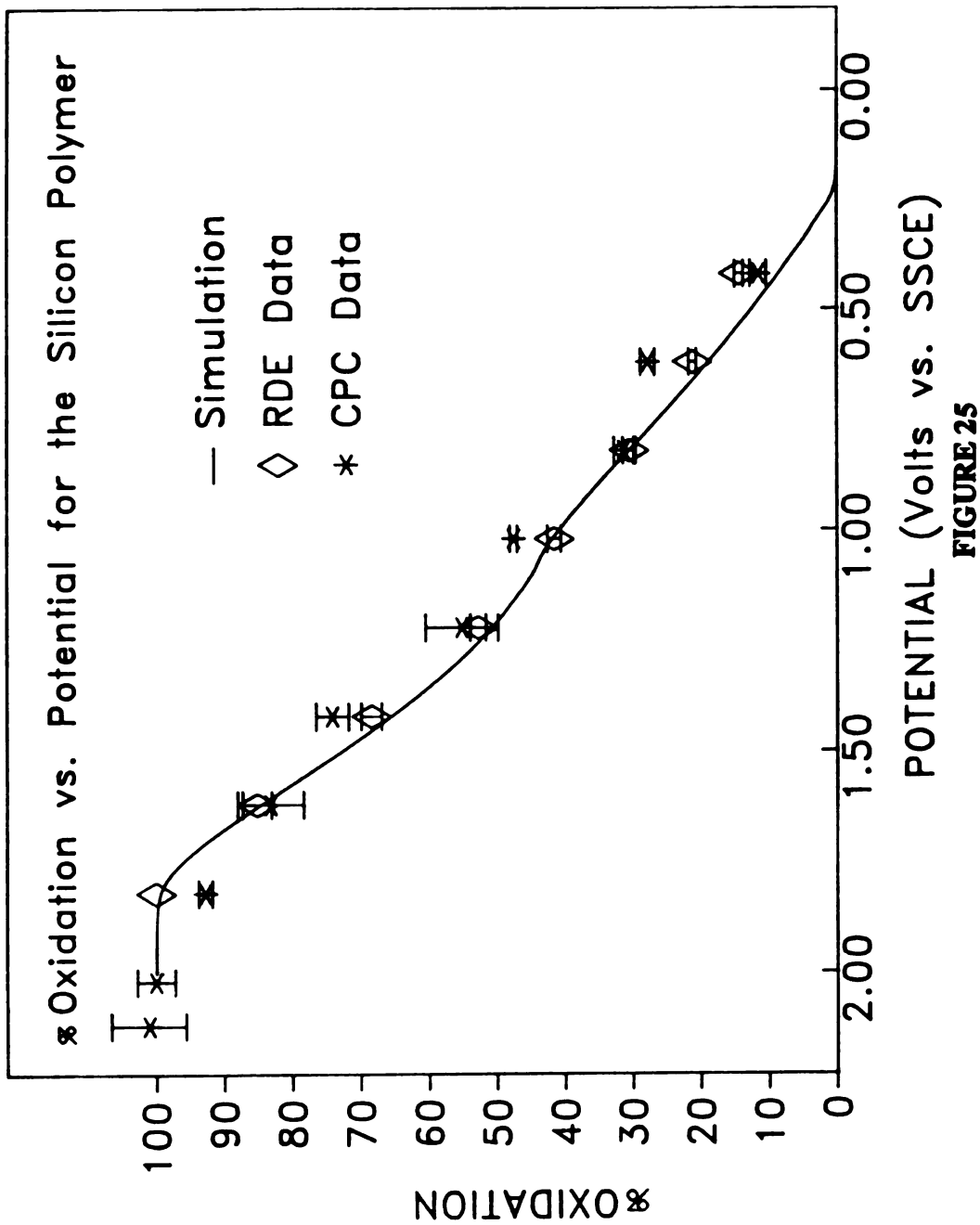
% Oxidation vs. Potential for the Silicon Polymer
— Simulation
◇ RDE Data
* CPC Data
%OXIDATION
100
90
80
70
60
50
40
30
20
10
0
2.00
1.50
1.00
0.50
0.00
POTENTIAL (Volts vs. SSCE)

FIGURE 25

hours to obtain a percent oxidation vs. potential profile of the polymer, while the RDE results were obtained in less than 1 hours.

The differential pulse voltammogram of the silicon polymer is very broad and unlike most voltammograms of normal redox couples, it is not very smooth. It is obvious that the redox states are too close together to resolve with this technique. A digital simulation utilizing the finite differences method, and oxidizing the polymer based on a sequential electron transfer model, provides information on the redox potential and distribution of states in the polymer. The simulation also provides information on the literature reported degree of polymerization, because it requires 25 sites to accurately model both the current as well as the potential response of the experimental DPV. The degree of polymerization calculated from the diffusion coefficient data also supports the degree of polymerization used for the digital simulations.

Potential applications of these materials will depend on the ability to shuttle charge in and out of the polymer. The determination of these rates of electron transfer over the entire range of band-filling could have a large effect on their uses in a number of fields. Preliminary results for reductive doping of the silicon phthalocyanine polymer have also been obtained. The reductive doping appears to be similar in most respects to the oxidative data. The percent reduction-potential curve occurs over a wide potential range very similar to that for the percent oxidation-potential curve. With both reduction and oxidation possible, a wide range of oxidation states is possible, and will provide numerous opportunities to study the physical and chemical properties over a

unprecedented range of band-filling. A great deal of information can be obtained on this particular system as a function of polymer oxidation or reduction. One example is the current dip at 1.00 V in the DPV voltammogram, this may be due to a reoganization in the polymer's redox states. Bulk samples can be prepared at specific levels of partial oxidation (or reduction), and spectroscopic measurements can be performed, to characterize the physical properties of the polymer at that degree of partial oxidation or reduction. Bulk samples can be characterized by a number of techniques, such as FTIR, conductivity, and EPR. These methods will provide information concerning the properties of the silicon polymer as a function of the degree of partial oxidation or reduction.

APPENDIX

APPENDIX A

The model utilized for the digital simulation of the DPV and CV current-potential responses is based on the assumption that each phthalocyanine ring is a redox active site, with its own unique standard potential (E^o_j). The oxidation of the polymer can be viewed as a system undergoing sequential electron transfer

$$R_n \overset{\rightarrow}{\leftarrow} R_{n-1}O_1 + e^- \qquad E^o_1 \qquad \text{A.1}$$

$$R_{n-1}O_1 \overset{\rightarrow}{\leftarrow} R_{n-2}O_2 + e^- \qquad E^o_2 \qquad \text{A.2}$$

$$R_{n-2}O_2 \overset{\rightarrow}{\leftarrow} R_{n-3}O_3 + e^- \qquad E^o_3 \qquad \text{A.3}$$

etc.

where R = reduced species, O = oxidized species and n = the length of the polymer. The polymer was taken to be 25 redox states (reference 1a, Vol. 1, chapter 5). The fractional concentration of any species at a given potential can be calculated from the potential dependant equilibrium constant (K_j) for that particular electron transfer event.

The fractional concentration of any species, $\alpha_n = R_n/C_T$ (where C_T is the concentration of the total number of redox active sites) is calculated from:

$$\alpha_o = \frac{1}{1 + K_1 + K_1K_2 + K_1K_2K_3 \ldots + K_1K_2K_3 \ldots K_n} \qquad \text{A.4}$$

Each individual equilibrium constant K_j is calculated from the Nernst equation: $K_j = \exp[(E-E^{\circ}_j)RT/n_jF]$. This model is exactly analogous to that used for the dissociation of a polyfunctional acid or base. This model works for both the oxidation as well as for the reduction of a multi-redox site polymer.

REFERENCES

1. (a) Skotheim, T.A., Ed. "Handbook of Conducting Polymers" (Dekker, New York 1986) Vols. 1-2. (b) Ferraro, J. R.; Williams, J.M., "Introduction to Synthetic Electrical Conductors", (Academic Press: New York, 1987). (c) Becker, J.Y.; Bernstein, J.; Bittner, S., Eds., Israel J. Chem., 1986, 27(4). (d) Skotheim, T. A., Ed. "Electroresponsive molecular and polymeric systems" (Dekker, New York, 1988), vol. 1. (e) Proceedings of the International Conference on Science and Technology of Synthetic Metals (ICSM '86), Synth. Met., 1987, 17. (f) Jerome, D.; Caron, L.G., Eds. "Low-Dimensional Conductors and Superconductors", Plenum: New York, 1987. (g) Proceedings of the International Conference on Science and Technology of Synthetic Metals (ICSM '88), Synth. Met., 1988-1989, 27-29 (h) A.J. Epstein, E.M. Conwell, Eds. "Proceeding of the International Conference on Low-Dimensional Conductors"; Boulder, Colorado, August 9-14, 1981. Mol. Cryst. Liq. Cryst. 77, 79, 83, 85, 86 Parts A-F (1981-1982). (i) Hanack, M.; Mitulla, K.; Pawlowski, G.; Subramanian, L. R. J. Organometallic Chem., 1981, 204 315-325.

2. (a) Chiang, C. K.; Fincher, C. R. Jr.; Park, Y. W.; Heeger, A. J.; Shirakawa, H.; Louis, E. J.; Gau, S. C.; MacDiarmid, A. G. Phys. Rev. Lett., 1977, 39, 1098. (b) Chiang, C. K.; Druy, M. A.; Gau, S. C.; Heeger, A. J.; Louis, E. J.; MacDiarmid, A. G.; Park, Y. W. J. Am. Chem. Soc., 1978, 100, 1013. (c) Ehrenfreund, E.; Rybaczewski, E. F.; Garito, A. F.; Heeger, A. J. Phys. Rev. Lett., 1972, 28, 873. (d) Ferraris, J.; Cowan, D. O.; Walatka, V.; Perlstein, J. H. J. Am. Chem. Soc., 1973, 95, 948.

3. (a) Duke, C. B. Synth. Met., 1987, 21, 5-12. (b) Inganas, O.; Lundstrom, I. Synth. Met., 1987, 21, 13-19. (c) MacDiarmid, A. G. Synth. Met., 1987, 21, 79-83. (d) Akhtar, M.; Weakliem, H. A.; Paiste, R. M.; Gaughan, K. Synth. Met., 1988, 26, 203-208.

4. (a) Cowan, D. O.; Wiygul, F. M. Chem. Eng. News, 1986, 64(29), 28-45. (b) Ward, M.W. "Electroanalytical Chemistry", Bard, A.J., Ed. (Dekker, New York, 1989) Vol. 16, 181-312. (c) Bryce, M.; Murphy, L. Nature, 1984, 309, 109. (d) Wudl, F. Acc. Chem

Res., 1984, 17(6), 227-232. (E) Williams, J.M. "Progress in Inorganic Chemistry", Lippard, S. J., Ed. (Wiley, New York, 1985), Vol 33, 183-220.

5. (a) Scrosati, B. Prog. Solid State Chem., 1988, 18(1), 1-77. (b) Wegner, G. Angew. Chem. Int. Ed. Eng., 1981, 20(4), 361-381. (c) Reynolds, J.R. Chemtech, 1988, 18(7), 440-447. (d) Miller, J.S., Ed. "Extended Linear Chain Compounds" (Plenum Press, New York, 1982), Vols. 1-3.

6. (a) Greene, R.L.; Street, G.B. Science, 1984, 226, 651-656.

7. (a) Hoffmann, R. Angew. Chem. Int. Ed., Eng., 1987, 26, 846. (b) Miller, J. S.; Epstein, A. J. "Progress in Inorganic Chemistry", Lippard, S. J., Ed. (Wiley, New York, 1985), Vol. 20, 1-151. (c) Duke, B. J.; O'Leary, B. J. Chem. Ed., 1988, 65(4), 319-321. (d) Duke, B. J.; O'Leary, B. J. Chem. Ed., 1988, 65(5), 379-383.

8. (a) Marks, T.J. Science, 1985, 227, 881-889.

9. (a) Diaz, A. F.; Lacroix, J. C., New J. Chem., 1988, 12(4), 171-180. (b) Wudl, F. Israel J. Chem., 1986, 27(4), 289-292.

10. (a) Diaz, A. F.; Logan, A. J. J. Electroanal. Chem., 1980, 111, 111-114. (b) Diaz, A. F.; Clark, T. C. J. Electroanal. Chem., 1980, 111, 115-117. (c) Diaz, A. F.; Castillo, J. I.; Logan, J. A.; Lee, W.-Y. J. Electroanal. Chem., 1981, 129, 115-132. (d) Diaz, A. F.; Martinez, A.; Kanazawa, K. K. J. Electroanal. Chem., 1981, 130, 181-187. (e) Bull, R. A.; Fan, F.-R. F.; Bard, A. J. J. Electrochem Soc., 1982, 129, 1009-1015. (f) Diaz, A. J.; Castillo, J.; Kanazawa, K. K.; Logan, J. A. J. Electroanal. Chem., 1982, 133, 233-239. (g) Tourillon, G.; Garnier, F. J. Electroanal. Chem., 1982, 135, 173-178. (h) Genies, E. M.; Bidan, G.; Diaz, A. F. J. Electroanal. Chem., 1983, 149, 101-113. (i) Waltman, R. J.; Bargon, J.; Diaz, A. J. J. Phys. Chem., 1983, 87, 1459-1463.

11. (a) Feldberg, S. W. J. Am. Chem. Soc., 1984, 106, 4671-4674, and references therein. (b) Murray, R. W., "Electroanalytical Chemistry", Bard, A. J., Ed. (Dekker, New York, 1984) vol 13.

12. (a) Miller, J. S.; Epstein, A. J. Angew. Chem. Int. Ed., Eng., 1987, 26(4), 287-293. (b) Conwell, E.M.; Howard, I. A. Synth. Met., 1986, 13, 71-85. (c) Epstein, A. J.; Kaufer, J. W.; Rommelmann, H.; Howard, I. A.; Conwell, E.M.; Miller, J. S.; Pouget, J. P.; Comes, R. Phys. Rev Lett., 1982, 49(14), 1037-1041. (d) Conwell, E.M.; Howard, I. A. Mol. Cryst. Liq. Cryst., 1985, 120, 51-58. (e) Epstein, A. J.; Bigelow, R. W.; Miller, J. S.; McCall, R. P.; Tanner, D. B. Mol. Cryst. Liq. Cryst., 1985, 120, 43-49. (f) Mazumdar, S.; Dixit, S. N.; Bloch, A. N. Mol. Cryst. Liq. Cryst., 1985, 120, 35-42.

13. (a) Diel, B. D.; Inabe, T.; Lyding, J. W.; Schoch, Jr, K. F.; Kannewurf, C. R.; Marks, T. J. J. Am. Chem. Soc., 1983, 105, 1551-1567. (b) Petersen, J. L.; Schramm, C. S.; Stojakovic, D. R.; Hoffman, B. M.; Marks, T. J. J. Am. Chem. Soc., 1977, 99, 286-288. (c) Schramm, C. S.; Scaringe, R. P.; Stojakovic, D. R.; Hoffman, B. M.; Ibers, J. A.; Marks, T. J. J. Am. Chem. Soc., 1980, 102, 6702-6713. (d) Diel,B. D.; Inabe, T.; Jaggi, N. K.; Lyding, J. W.; Schneider, O.; Hanack, M.; Kannewurf, C. R.; Marks, T. J.; Schwartz, L. H. J. Am. Chem. Soc., 1984, 106, 3207-3214. (e) Inabe, T.; Gaudiello, J. G.; Moguel, M. K.; Lyding, J. W.; Burton, R. L.; McCarthy, W. J.; Kannewurf, C. R.; Marks, T. J. J. Am. Chem. Soc., 1986, 108, 7595-7608. (f) Marks, T. J.; Schoch, K. F. Jr.; Kundalkar, B. R. Synth. Met., 1979-1980, 1, 337. (g) Brant, P.; Nohr, R. S.; Wynne, K. J.; Weber, D. C. Mol. Cryst. Liq. Cryst., 1982, 81, 255. (h) Dirk, C. W.; Inabe, T.; Schoch, Jr, K. F.; Marks, T. J. J. Am. Chem. Soc., 1983, 105, 1539-1550. (i) Nohr, R. S.; Kuznesof, P. M.; Wynne, K. J.; Kenney, M. E.; Siebenmann, P. G. J. Amer. Chem. Soc., 1981, 103, 4371-4377.

14. (a) Ofer, D.; Wrighton, M. S. J. Am. Chem. Soc., 1988, 110, 4467-4468.

15. (a) Gaudiello, J. G.; Marcy, H. O.; McCarthy, W. J.; Moguel, M. K.; Kannewurf, C. R.; Marks, T. J. Synth. Met., 1986, 15, 115-128. (b) Gaudiello, J. G.; Almeida, M.; Marks, T. J.; McCarthy, W. J.; Butler, J. C.; Kannewurf, C. R. J. Phys. Chem., 1986, 90, 4917-4920. (c) Almeida, M.; Gaudiello, J. G.; Butler, J. C.; Marcy, H. O.; Kannewurf, C. R.; Marks, T. J. Synth. Met., 1988, 27, 261-266. (d) Kellogg, G. E.; Gaudiello, J. G.; Schlueter, J. A.; Tetrick, S. M.; Marks, T. J.; Marcy, H. O.; McCarthy, W.

J.; Kannewurf, C. R. Synth. Met., 1989, 29, F15-F24. (e) Gaudiello, J. G.; Kellogg, G. E.; Tetrick, S. M.; Marks, T. J. J. Am. Chem. Soc., 1989, 111, 5259-5271. (f) Almeida, M.; Gaudiello, J. G.; Kellogg, G. E.; Tetrick, S. M.; Marcy, H. O.; McCarthy, W. J.; Butler, J. C.; Kannewurf, C. R.; Marks, T. J. J. Am. Chem. Soc., 1989, 111, 5271-5284.

16. (a) Hanack, M.; Lange, A.; Rein, M.; Behnisch, R.; Renz, G.; Leverenz, A. Synth. Met., 1989, 29, F1-F8. (b) Hanack, M. Israel J. Chem., 1985, 25, 205-209.

17. (a) Metz, J.; Pawlowowski, G.; Hanack, M. Z. Naturforsch., 1983, 38b(3), 378-382. (b) Hanack, M.; Datz, A.; Fay, R.; Fishcher, K.; Keppeler, U.; Koch, J.; Metz, J.; Mezger, M.; Schneider, O.; Schulze, H., "Handbook of Conducting Polymers", Skotheim, T. A., Ed. (Dekker, New York, 1986) vol. 1, and references therein. (c) Hanack, M.; Metz, J.; Pawlowski, G. Chem. Ber., 1982, 115, 2836-2853.

18. (a) Hanack, M.; Leverenz, A. Synth. Met., 1987, 22, 9-14.

19. (a) Simic-Glavaski, B.; Tanaka, A. A.; Kenney, M. E.; Yeager, E. J. Electroanal. Chem., 1987, 229, 285-296. (b) Mezza, T. M.; Armstrong, N. R.; Ritter, G. W.; Iafalice, J. P.; Kenney, M. E. J. Electroanal. Chem., 1982, 137, 227. (c) Wheeler, B. L.; Nagasubramanian, G.; Bard, A. J.; Schechtman, L. A.; Dininny, D. R.; Kenney, M. E. J. Amer. Chem. Soc., 1984, 106, 7404. (d) DeWulf, D. W.; Leland, J. K.; Wheeler, B. L.; Bard, A. J.; Batzel, D. A.; Dininny, D. R.; Kenney, M. E. Inorg. Chem., 1987, 26, 266. (e) Ciliberto, E.; Doris, K. A.; Pietro, W. J.; Reisner, G. M.; Ellis, D. E.; Fragala, I.; Herbstein, F. H.; Ratner, M. A.; Marks, T. J. J. Amer. Chem. Soc., 1984, 106, 7748.

20. (a) Elsenbaumer, R. L.; Jen, K. Y.; Ododi, R. Synth. Met., 1986, 15, 169-174. (b) Patil, A. O.; Ikenoue, Y.; Wudl, F.; Heeger, A. J. J Am. Chem. Soc., 1987, 109, 1858-1859. (c) Patil, A. O.; Ikenoue, Y.; Wudl, F.; Heeger, A. J. Synth. Met., 1987, 20, 151, and references therein. (d) Patil, A. O.; Ikenove, Y.; Basecu, N.; Colaneri, N.; Chen, J.; Wudl, F.; Heeger, A. J. Synth. Met., 1987, 20, 151-159. (e) Rughooputh, S. D. D. V.; Nowak, M.; Hotta, S.; Heeger, A. J.; Wudl, F. Synth. Met., 1987,

21, 41-50. (f) Sato, M-A.; Tanaka, S.; Kaeriyama, K. Synth. Met., 1987, 18, 229-232. (g) Hotta, S.; Rughooputh, S. D. D. V.; Heeger, A. J.; Wudl, F. Macromolecules, 1987, 20, 212-215.

21. (a) Schriver, D. E. "The Manipulation of Air-Sensitive Compounds"; (McGraw-Hill, New York, N.Y. 1969).

22. (a) Smith, W. H.; Bard, A. J. J. Am. Chem. Soc., 1975, 97, 5203-5210.

23. (a) Adams, R. N., "Electrochemistry at Solid Electrodes" (Marcel Dekker, New York, 1969) and references therein.

24. (a) Bard, A. J.; Faulkner, L. R., "Electrochemical Methods" (Wiley, New York, 1980). (b) Rieger, P. H., "Electrochemistry" (Prentice-Hall, Englewood Cliffs, N. J. 1987). (c) Kissenger, P. T.; Heineman, W. R., Eds. "Laboratory Techniques in Electroanalytical Chemistry", (Marcel Dekker, New York, 1984). (d) Harrar, J. E. "Electroanalytical Chemistry", Bard, A.J., Ed. (Dekker, New York, 1975) Vol. 8, 1-167.

25. (a) Couves, J. W.; Wright, J. D. Synth. Met., 1989, 29, F77-F82.

26. (a) Brown, G. H.; Meyer, T. J.; Cowan, D. O.; LeVanda, C.; Kaufman, F.; Roling, P. V.; Rausch, M. D. Inorg. Chem., 1975, 14, 506-511. (b) Brennam, D. E.; Geiger, W. E. J. Am. Chem. Soc., 1979, 101, 3399-3400. (c) Flanagan, J. B.; Margel, S.; Bard, A. J.; Anson, F. C. J. Am. Chem. Soc., 1979, 100, 4248-4253.

27. (a) Su, W. P.; Schrieffer, J. R.; Heeger, A. J. Phys. Rev. Lett., 1979, 42, 1698. (b) Rice, M. J. Phys. Lett., 1979, A-71, 152. (c) Schrieffer, J. R. Mol. Cryst. Liq. Cryst., 1981, 77, 201.

28. Tanford, C, "Physical Chemistry of Macromolecules", (Wiley, New York, 1961).

29. (a) Feldberg, S. W. "Electroanalytical Chemistry"; Bard, A. J. Ed.,(Marcel Dekker, New York, 1964) Vol 3, 271. (b) Prater, K. B., "Computers in Chemistry and Instrumentation"; Mattson, J. S.; Mark, H. B.; MacDonald, H. C. Eds., (Marcel Dekker, New

York, 1972) Vol 2. (c) Malloy, J. T. "Laboratory Techniques in Electroanalytical Chemistry", Kissenger, P. T.; Heineman, W. R. Eds.,(Marcel Dekker, New York, 1984). (d) Britz, D. "Digital Simulations in Electrochemistry, Lecture notes in Chemistry" (Springer-Verlag, Heidleberg, 1981).